

BSC	Design Calculation or Analysis Cover Sheet	1. QA: QA
		2. Page 1 of 54

3. System Subsurface	4. Document Identifier 000-00C-SSE0-00800-000-00A-B
5. Title Emplacement Pallet Lift and Degraded Static Analysis	
6. Group Thermal Structural Analysis	
7. Document Status Designation <input type="checkbox"/> Preliminary <input checked="" type="checkbox"/> Committed <input type="checkbox"/> Confirmed <input type="checkbox"/> Cancelled/Superseded	

8. Notes/Comments Jason Viggato is an approved checker according to IOM number 0726071450 from Michael Anderson.

Attachments	Total Number of Pages
See Section 5	N/A

RECORD OF REVISIONS

9. No.	10. Reason For Revision	11. Total # of Pgs.	12. Last Pg. #	13. Originator (Print/Sign/Date)	14. Checker (Print/Sign/Date)	15. EGS (Print/Sign/Date)	16. Approved/Accepted (Print/Sign/Date)
00A	Initial Issue This document supersedes "Emplacement Pallet Lift", 000-00C-TEP0-00100-000-00A and "Degraded Emplacement Pallet Static", 000-00C-TEP0-00200-000-00A. This document is issued to reflect the latest waste package and emplacement pallet design.	54	54	Nakachew A. Alemu <i>[Signature]</i> 08/06/07	Jason Viggato <i>[Signature]</i> 8/6/07	Jason Viggato <i>[Signature]</i> 8/6/07	Michael J. Anderson <i>[Signature]</i> 8/6/07
00B	Administrative wording change. Pages 9 and 24 only.			Nakachew A. Alemu <i>[Signature]</i> 08/10/07			Michael J. Anderson <i>[Signature]</i> 8/10/07

DISCLAIMER

The calculations contained in this document were developed by Bechtel SAIC Company, LLC. (BSC) and are intended solely for the use of BSC in its work for the Yucca Mountain Project.

CONTENTS

	Page
1 PURPOSE.....	7
2 REFERENCES	7
2.1 PROJECT PROCEDURES/DIRECTIVES	7
2.2 DESIGN INPUTS.....	7
2.3 DESIGN CONSTRAINTS	10
2.4 DESIGN OUTPUTS.....	10
3 ASSUMPTIONS	11
3.1 ASSUMPTIONS REQUIRING VERIFICATION.....	11
3.2 ASSUMPTIONS NOT REQUIRING VERIFICATION	11
4 METHODOLOGY	13
4.1 QUALITY ASSURANCE.....	13
4.2 USE OF SOFTWARE	13
4.3 STRESS ANALYSIS APPROACH	14
5 LIST OF ATTACHMENTS.....	15
6 BODY OF CALCULATION	16
6.1 MATERIAL PROPERTIES	16
6.2 PRE-CLOSURE LIFT ACCELERATION.....	18
6.3 POST-CLOSURE THICKNESS REDUCTION	18
6.4 FINITE ELEMENT REPRESENTATIONS	18
7 RESULTS AND CONCLUSIONS	23
7.1 ANALYSIS CRITERIA	23
7.2 CONCLUSIONS	25
7.3 EP LIFT ANALYSIS AT RT.....	27
7.4 EP LIFT ANALYSIS AT 250°C	35
7.5 DEGRADED EP STATIC ANALYSIS AT RT	41
7.6 DEGRADED EP STATIC ANALYSIS AT 150°C.....	47

FIGURES

	Page
Figure 6-1 EP and OCB Finite Element Model used for the Analysis.....	19
Figure 6-2 EP Model used for Lift Analysis at RT and 250 °C.....	20
Figure 6-3 EP Model used for Degraded Static Analysis at RT and 150°C.....	21
Figure 6-4 An Isometric View of Quarter Symmetry EP Model with Contact Surface.....	22
Figure 7-1 Average Bearing Stress S_b [Pa] of Plate 6 for EP Lift Analysis at RT.....	27
Figure 7-2 Average Maximum Stress Intensity, SI [Pa] of Plate 6 for EP Lift Analysis at RT	28
Figure 7-3 Average Maximum Tensile Stress, SI [Pa] of Plate 6 for EP Lift Analysis at RT	29
Figure 7-4 Maximum Stress Intensity SI [Pa] of Plate 9 for EP Lift Analysis at RT.....	30
Figure 7-5 Bearing Stress S_b [Pa] of Plate 9 for EP Lift Analysis at RT	31
Figure 7-6 Maximum Tensile Stress, SI [Pa] of Plate 9 for EP Lift Analysis at RT.....	32
Figure 7-7 Average Bearing Stress S_b [Pa] of the OCB for EP Lift Analysis at RT.....	33
Figure 7-8 Average Maximum Tensile Stress, SI [Pa] of the OCB for EP Lift Analysis at RT	34
Figure 7-9 Average Bearing Stress S_b [Pa] of Plate 6 for EP Lift Analysis at 250°C.....	35
Figure 7-10 Average Stress Intensity SI [Pa] of Plate 6 for EP Lift Analysis at 250°C	36
Figure 7-11 Average Maximum Tensile Stress, SI [Pa] of Plate 6 for EP Lift Analysis at 250°C.....	37
Figure 7-12 Bearing Stress S_b [Pa] of Plate 9 for EP Lift Analysis at 250 °C.....	38
Figure 7-13 Maximum Stress Intensity SI [Pa] of Plate 9 for EP Lift Analysis at 250 °C.....	39
Figure 7-14 Maximum Tensile Stress SI [Pa] of OCB for EP Lift Analysis at 250 °C	40
Figure 7-15 Average Bearing Stress S_b [Pa] of OCB for EP Lift Analysis at 250 °C	41
Figure 7-16 Maximum Stress Intensity, SI [Pa] of the EP for Degraded EP Static Analysis at RT.....	42
Figure 7-17 Average Bearing Stress, S_b [Pa] of Plate 6 for Degraded EP Static Analysis at RT	43
Figure 7-18 Maximum Tensile Stress, SI [Pa] on the EP for the Degraded EP Static Analysis at RT...	44
Figure 7-19 Bearing Stress, S_b [Pa] on the OCB for Degraded EP Static Analysis at RT.....	45
Figure 7-20 Maximum Tensile Stress SI [Pa] on OCB for Degraded EP Static Analysis at RT	46
Figure 7-21 Maximum Stress Intensity SI [Pa] of the EP for Degraded EP Static Analysis at 150°C....	47
Figure 7-22 Average Bearing Stress, S_b [Pa] of Plate 6 for Degraded EP Static Analysis at 150°C	48
Figure 7-23 Maximum Tensile Stress, SI [Pa] on the EP for the Degraded EP Static Analysis at 150°C	49
Figure 7-24 Maximum Tensile Stress, SI [Pa] on Plate 6 for the Degraded EP Static Analysis at 150°C	50
Figure 7-25 Maximum Tensile Stress, SI [Pa] on Plate 1 for the Degraded EP Static Analysis at 150°C	51
Figure 7-26 Bearing Stress, S_b [Pa] of Plate 1 for Degraded EP Static Analysis at 150°C.....	52
Figure 7-27 Maximum Tensile Stress, SI [Pa] of OCB for Degraded EP Static Analysis at 150°C.....	53
Figure 7-28 Average Bearing Stress, S_b [Pa], of OCB for Degraded EP Static Analysis at 150°C	54

TABLES

	Page
Table 5-1 Table of Attachments	15
Table 5-2 Attachment I Files	15
Table 7-1 ASME Allowable Design Stress Intensity Values	24
Table 7-2 Stress Results Table for EP Lift Analysis While Loaded With TAD WP	25
Table 7-3 Stress Results Table for Degraded EP Static Analysis While Loaded With TAD WP	26

ACRONYMS

ASME	American Society of Mechanical Engineers
ASM	American Society for Metals
ASTM	American Society of Testing Materials
BSC	Bechtel SAIC Company, LLC
DOE	U.S. Department of Energy
EP	Emplacement Pallet
FEA	Finite Element Analysis
FER	Finite Element Representation
OCB	Outer Corrosion Barrier
RT	Room Temperature
TAD	Transportation, Aging and Disposal
TEV	Transport and Emplacement Vehicle
WP	Waste Package
YMP	Yucca Mountain Project

1 PURPOSE

The two-fold purposes of this calculation are: (1) to determine the structural response of the Emplacement Pallet (EP) during lift while loaded with the heaviest waste package (WP), (TAD-Transportation, Aging and Disposal) (References 2.2.18 to 2.2.20) and (2) to determine the structural response of the EP with reduced thickness while loaded with the TAD WP and rested on the invert after 10,000 years of corrosion degradation. The scope of this document is limited to calculate and document ASME Code compliance for plate-type supports; an elastic analysis based on the design stress intensity (SI), and bearing stress (Sb), values within allowable limits of the allowable design stress intensity (Sm) and yield strength (Sy). The document will also report the maximum tensile stress on the surfaces of the structural components of the WP OCB and the EP are in compliance with the post-closure requirement criteria (Reference 2.2.32, Table 1, Item 08-05). The stress results are reported in terms of maximum stress intensity (SI), bearing stress (Sb), and the maximum principal stresses (SI).

This calculation is intended for use in support of the design activities for the Emplacement Pallet (EP), the Waste Package (WP) and Drip Shield for the License Application (LA), and is performed by the Thermal Structural Analysis Group.

2 REFERENCES

2.1 PROJECT PROCEDURES/DIRECTIVES

- 2.1.1 EG-PRO-3DP-G04B-00037, Rev. 9. *Calculations and Analyses*. Las Vegas, Nevada: Bechtel SAIC Company. ACC: [ENG.20070717.0004](#)
- 2.1.2 BSC 2007. *Quality Management Directive*. QA-DIR-10, Rev.001. Las Vegas, Nevada: Bechtel SAIC Company. ACC: [DOC.20070330.0001](#).
- 2.1.3 IT-PRO-0011, Rev.005. *Software Management*. Las Vegas, Nevada: Bechtel SAIC Company. ACC: [DOC.20070521.0001](#).
- 2.1.4 ORD (Office of Repository Development) 2007. *Repository Project Management Automation Plan*. 000-PLN-MGR0-00200-000, Rev. 00E. Las Vegas, Nevada: U.S. Department of Energy, Office of Repository Development. ACC: [ENG.20070326.0019](#).

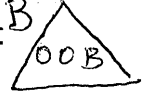
2.2 DESIGN INPUTS

- 2.2.1 BSC 2006. *Basis of Design for the TAD Canister-Based Repository Design Concept*. 000-3DR-MGR0-00300-000-000. Las Vegas, Nevada: Bechtel SAIC Company. ACC: [ENG.20061023.0002](#).
- 2.2.2 BSC (Bechtel SAIC Company) 2003. *Design and Engineering, Emplacement Pallet Configuration*. 000-M00-TEP0-00102-000-00A. Las Vegas, Nevada: Bechtel SAIC Company. ACC: [ENG.20031006.0004](#).

- 2.2.3 BSC (Bechtel SAIC Company) 2004. Design and Engineering, Emplacement Pallets Assembly for License Application. 000-M00-SSE0-00301-000-00A. Las Vegas, Nevada: Bechtel SAIC Company. ACC: [ENG.20040224.0005](#).
- 2.2.4 BSC (Bechtel SAIC Company) 2004. Design and Engineering, Emplacement Pallet Assembly Exploded. 000-M00-SSE0-00302-000-00A. Las Vegas, Nevada: Bechtel SAIC Company. ACC: ENG.20040224.0006.
- 2.2.5 BSC (Bechtel SAIC Company) 2004. Design and Engineering, Emplacement Pallet Waste Package Support Assembly Exploded. 000-M00-SSE0-00303-000-00A. Las Vegas, Nevada: Bechtel SAIC Company. ACC: [ENG.20040224.0007](#).
- 2.2.6 BSC (Bechtel SAIC Company) 2004. Design and Engineering, Emplacement Pallet Assembly Plate 1. 000-M00-SSE0-00304-000-00A. Las Vegas, Nevada: Bechtel SAIC Company. ACC: [ENG.20040224.0008](#).
- 2.2.7 BSC (Bechtel SAIC Company) 2004. Design and Engineering, Emplacement Pallet Assembly Plate 2. 000-M00-SSE0-00305-000-00A. Las Vegas, Nevada: Bechtel SAIC Company. ACC: [ENG.20040224.0009](#).
- 2.2.8 BSC (Bechtel SAIC Company) 2004. Design and Engineering Emplacement Pallet Assembly Plate 3. 000-M00-SSE0-00306-000-00A. Las Vegas, Nevada: Bechtel SAIC Company. ACC: [ENG.20040224.0010](#).
- 2.2.9 BSC (Bechtel SAIC Company) 2004. Design and Engineering Emplacement Pallet Assembly Plate 4. 000-M00-SSE0-00307-000-00A. Las Vegas, Nevada: Bechtel SAIC Company. ACC: ENG.20040224.0011.
- 2.2.10 BSC (Bechtel SAIC Company) 2004. Design and Engineering Emplacement Pallet Assembly Plate 5. 000-M00-SSE0-00308-000-00A. Las Vegas, Nevada: Bechtel SAIC Company. ACC: ENG.20040224.0012.
- 2.2.11 BSC (Bechtel SAIC Company) 2004. Design and Engineering, Emplacement Pallet Assembly Plate 6. 000-M00-SSE0-00309-000-00A. Las Vegas, Nevada: Bechtel SAIC Company. ACC: [ENG.20040224.0013](#).
- 2.2.12 BSC (Bechtel SAIC Company) 2004. Design and Engineering, Emplacement Pallet Assembly Plate 7. 000-M00-SSE0-00310-000-00A. Las Vegas, Nevada: Bechtel SAIC Company. ACC: ENG.20040224.0014.
- 2.2.13 BSC (Bechtel SAIC Company) 2004. Design and Engineering, Emplacement Pallet Assembly Plate 8. 000-M00-SSE0-00311-000-00A. Las Vegas, Nevada: Bechtel SAIC Company. ACC: ENG.20040224.0015.
- 2.2.14 BSC (Bechtel SAIC Company) 2004. Design and Engineering, Emplacement Pallet Assembly Plate 9. 000-M00-SSE0-00312-000-00A. Las Vegas, Nevada: Bechtel SAIC Company. ACC: ENG.20040224.0016.

08/16/07

na

Emplacement Pallet Lift and Degraded Static Analysis

000-00C-SSE0-00800-000-00A

- 2.2.15 BSC (Bechtel SAIC Company) 2004. Design and Engineering, Emplacement Pallet Assembly Tube 1. 000-M00-SSE0-00313-000-00A. Las Vegas, Nevada: Bechtel SAIC Company. ACC: ENG.20040224.0017.
- 2.2.16 BSC (Bechtel SAIC Company) 2004. Design and Engineering, Emplacement Pallet Assembly Tube 2. 000-M00-SSE0-00314-000-00A. Las Vegas, Nevada: Bechtel SAIC Company. ACC: ENG.20040224.0018.
- 2.2.17 BSC (Bechtel SAIC Company) 2004. Design and Engineering, Emplacement Pallet Assembly Tube 3. 000-M00-SSE0-00315-000-00A. Las Vegas, Nevada: Bechtel SAIC Company. ACC: ENG.20040224.0019.
- 2.2.18 BSC (Bechtel SAIC Company) 2007. *TAD Waste Package Sketch*. 000-MWK-DSC0-00101-000-00B. Las Vegas, Nevada: Bechtel SAIC Company. ACC: ENG.20070226.0033.
- 2.2.19 BSC (Bechtel SAIC Company) 2007. *TAD Waste Package Sketch*. 000-MWK-DSC0-00102-000-00B. Las Vegas, Nevada: Bechtel SAIC Company. ACC: ENG.20070226.0034.
- 2.2.20 BSC (Bechtel SAIC Company) 2007. *TAD Waste Package Sketch*. 000-MW0-DSC0-00103-000-00B. Las Vegas, Nevada: Bechtel SAIC Company. ACC: ENG.20070226.0035.

2.2.22 ~~2.2.21~~ Not Used.

2.2.21 ~~2.2.22~~ ASME (American Society of Mechanical Engineers) 2001. 2001 ASME Boiler and Pressure Vessel Code (includes 2002 addenda). New York, New York: American Society of Mechanical Engineers. TIC: 251425



na

08/10/07

- 2.2.23 ASTM (American Society for Testing and Materials) G 1-90 (Reapproved 1999). 1999. Standard Practice for Preparing, Cleaning, and Evaluating Corrosion Test Specimens. West Conshohocken, Pennsylvania: American Society for Testing and Materials. TIC: 238771
- 2.2.24 BSC (Bechtel SAIC Company) 2006. *IED Emplacement Pallet*. 800-IED-SSE0-00201-000-00B. Las Vegas, Nevada: Bechtel SAIC Company. ACC: ENG.20070608.0007.
- 2.2.25 Roark, R.J. and Young, W.C. 1975. *Formulas for Stress and Strain*. 5th Edition. New York, New York: McGraw-Hill. TIC: 240746. ISBN: 0-07-053031-9
- 2.2.26 ASM (American Society for Metals) 1980. *Properties and Selection: Stainless Steels, Tool Materials and Special-Purpose Metals*. Volume 3 of *Metals Handbook*. 9th Edition. Benjamin, D., ed. Metals Park, Ohio: American Society for Metals. TIC: 209801. ISBN: 0-87170-009-3
- 2.2.27 BSC 2007. *Waste Package Masses*. 000-00C-MGR0-01100-000-00D. Las Vegas, Nevada: Bechtel SAIC Company. ACC: ENG. ENG.20070402.0002.
- 2.2.28 ANSYS V. 8.0. 2004. HP-UX 11.0, HP-UX 11.22, SunOS 5.8. STN: 10364-8.0-00. [DIRS 170070]

- 2.2.29 DOE (U.S. Department of Energy) 2004. *Validation Test Report for: ANSYS V8.0*. Document Number 10364-VTR-8.0-00. Las Vegas, Nevada: U.S. Department of Energy Office of Repository Development. ACC: [MOL.20040422.0376](#). [DIRS 171758]
- 2.2.30 BSC (Bechtel SAIC Company) 2007. *Thermal Evaluation for the 5-DHLW/DOE SNF and TAD Waste Package in the TEV* 800-00C-DS00-00100-000-00A. Las Vegas, Nevada: Bechtel SAIC Company. ACC: [ENG.20070731.0043](#)
- 2.2.31 Avallone, E.A and Buameister, T. III, eds 1987. *Marks Standard Handbook for Mechanical Engineers*. 9th Edition. New York, New York: McGraw-Hill. TIC: [206891](#). ISBN: 0-07-004127-X
- 2.2.32 BSC (Bechtel SAIC Company) 2007. *Postclosure Modeling and Analyses Design Parameters*. TDR-MGR-MD-000037 REV 01. Las Vegas, Nevada: Bechtel SAIC Company. ACC: [ENG.20070613.0002](#)
- 2.2.33 Mecham, D.C., ed. 2004. *Waste Package Component Design Methodology Report*. 000-30R-WIS0-00100-000-002. Las Vegas, Nevada: Bechtel SAIC Company. ACC: [ENG.20040713.0003](#).

2.3 DESIGN CONSTRAINTS

None.

2.4 DESIGN OUTPUTS

This document was prepared to support the License Application. The outputs of this document will be used in the Emplacement Pallet and Waste Package Design Report.

3 ASSUMPTIONS

3.1 ASSUMPTIONS REQUIRING VERIFICATION

- 3.1.1 The dimensions, masses and materials of the Emplacement Pallet and TAD Waste Package used in the development of this calculation correspond to drawings and sketches of References 2.2.2 through 2.2.20 are assumed to be the same as the final definitive design. The rationale for this assumption is that the designs of References 2.2.2 through 2.2.20 are created for the License Application (LA). This assumption is used in Section 6.4 and will require verification at completion of the final definitive design.

3.2 ASSUMPTIONS NOT REQUIRING VERIFICATION

- 3.2.1 Since the room temperature (RT) (21 °C (70 °F)) Poisson's ratio of Alloy 22 is not published in traditional sources, the Poisson's ratio of ASME SB-443 [UNS N06625], hereinafter termed Alloy 625, is assumed for Alloy 22. The chemical composition of Alloy 22 and Alloy 625 are similar since they are both 600 Series nickel-base alloys (Reference 2.2.21, Section II, Part B, SB-575, Table 1 and Reference 2.2.26, p. 143, respectively). Therefore, the difference in their Poisson's ratio is expected to be small. The rationale for this presumption is that Reference 2.2.26, pages 141, 143 and 145 indicate small difference in RT Poisson's ratio values for the 600 Series nickel-base alloy family:

$$\begin{aligned}\text{Alloy 600 [UNS N06600]} &= 0.290 \\ \text{Alloy 625 [UNS N06625]} &= 0.278 \\ \text{Alloy 690 [UNS N06690]} &= 0.289\end{aligned}$$

The impact on stress results of small differences in Poisson's ratio is anticipated to be negligible. The rationale for this assumption is that Reference 2.2.25, Table 26, p. 392 stress formulas for rectangular plate, all edges fixed indicates insensitivity to Poisson's ratio. For a rectangular plate, fixed at all edges with a uniform load applied over a small concentric circle of radius r_0 , the maximum bending stress on the plate is proportional to the Poisson's ratio, ν , through the term $(1 + \nu)$ (Reference 2.2.25, Table 24, p. 392, Case 8b). Using the lowest and highest values of the three 600 Series nickel-base alloy ν values, 0.278 and 0.290, the difference in maximum bending stress values, all things being equal except ν , is 0.93%, which is less than 1%. Therefore, further verification of this assumption is not required. This assumption is used in Section 6.1.

- 3.2.2 The friction coefficients for contacts occurring between the materials used in this calculation are not published in traditional sources. It is, therefore, assumed that the dynamic (sliding) friction coefficient is 0.4 for all contacts. The rationale for this assumption is that this friction coefficient represents a reasonable lower bound value for most metal-on-metal contacts (Reference 2.2.31, Table 3.2.1, page 3-26). This assumption is used in Section 6.4.

- 3.2.3 The TAD WP is used in the Finite Element Representation (FER) (Reference 2.2.18 to 2.2.20). The exact mass and geometry of the TAD WP is simplified for the purpose of this calculation. A quarter model of the OCB is used to represent the TAD WP. The density of the OCB model is then back calculated using the quarter mass of the TAD WP, 18377.25 kg and the volume of the OCB model. The rationale for this assumption is that the simplification will conserve CPU processing time without compromising the desired structural analysis. Also the structural response of the internal components of the TAD WP is not in the scope of this calculation. This assumption is used in Section 6.4 and does not require verification.
- 3.2.4 A quarter symmetry model of the EP is used in the FER for both the lift and the degraded analyses. Some dimensions (References 2.2.2 to 2.2.17) of the structural components of the EP are rounded-off for modeling purposes. This simplification is expected to have no effect on the structural analysis of the EP. The rationale for this assumption is that the round-offs are made for components, which are not critical to the structural analysis and will help to conserve computing time while preserving features relevant to the structural calculation. This assumption is used in Section 6.4 and will not require verification.
- 3.2.5 For the degraded EP static load analysis, it is assumed that the thickness of Alloy 22 components of the EP will degraded by 2.56 mm after 10,000 years of corrosion. The rationale for this assumption is that Reference 2.2.24 provides an upper bound value of corrosion rate of 256 nm/year for Alloy 22 and 150 nm/year for 316 SS. Since the EP is composed of components made from Alloy 22 and 316 SS, and Reference 2.2.32, Table 1, Item 08-03 d) and e) requires at least 2 mm of corrosion allowance; the largest corrosion rate of 2.56 mm is used. This will provide the calculation with a conservatively bounded result of degradation with regards to material thickness. This assumption does not require verification and used in Section 6.3.
- 3.2.6 For the EP lift analysis, the lift acceleration used for the EP and TAD WP assembly is 1 m/s^2 , (total upward acceleration being 10.81 m/s^2 including gravity). The rationale for this assumption is that this value conservatively represents the lifting of the EP by the TEV and bounds the lifting strength for the emplacement pallet. This assumption does not require verification and used in Sections 6.2 and 6.4.
- 3.2.7 The Poisson's ratio and density at elevated temperature are not published in traditional sources for Alloy 22 and 316 SS. The RT Poisson's ratio and density are assumed for these materials. The impact of using RT Poisson's ratio and density is anticipated to be small. The rationale is that the temperature sensitivities of these material properties are expected to be small and small variations will have negligible effect on the calculation's stress results. This assumption is consistent with Section 5.2.8.6 of Reference 2.2.33. This assumption is used in Section 6.1.

4 METHODOLOGY

4.1 QUALITY ASSURANCE

This calculation is performed in accordance with EG-PRO-3DP-G04B-00037, *Calculations and Analyses* (Reference 2.1.1). The Emplacement Pallets are classified as important to safety and important to waste isolation (Reference 2.2.1, Sec 8.1.2). Therefore, this document is subject to requirements of the BSC *Quality Management Directive* (Reference 2.1.2) and the approved version is designated as QA: QA.

4.2 USE OF SOFTWARE

The finite element analysis code used for this calculation is ANSYS V8.0 (Reference 2.2.28), which is identified by the Software Tracking number 10364-8.0-00. Usage of ANSYS V8.0 in this calculation constitutes Level 1 software usage, as defined in IT-PRO-0011 (Reference 2.1.3, Attachment 12). ANSYS V8.0 is qualified, baselined, and listed in the current *Qualified and Controlled Software Report*, as well as the *Repository Project Management Automation Plan* (Reference 2.1.4 Table 6-1).

Computations using ANSYS V8.0 software were executed on the following Hewlett-Packard (HP) 9000 Series workstations running operating system HP-UX 11.00:

Central Processing Unit (CPU) Name: Rosebud, Civilian Radioactive Waste Management System Management (CRWMS M&O) Tag Number: 150689

CPU Name: Milo, CRWMS M&O Tag Number: 151665

CPU Name: Oliver, CRWMS M&O Tag Number: 150688

The ANSYS V8.0 evaluations performed in this calculation are fully within the range of the validation performed for ANSYS V8.0 (Reference 2.2.29). Therefore, ANSYS V8.0 is appropriate for the structural analyses performed in this calculation. Access to, and use of, the code for this calculation is granted by *Software Configuration Management* in accordance with the appropriate procedures. The details of the ANSYS analyses are described in Section 6.4 and the results are presented in Sections 7.2 to 7.6 of this calculation.

The commercially available TrueGrid V2.3.0 (Software Tracking Number 610418-2.2.0-00) a mesh generating code, hereinafter referred to as “TrueGrid”, is used in this calculation solely to mesh geometric representations of the EP and the OCB for the simulations and analyses, TrueGrid usage is Level 2 status as defined in Reference 2.1.3, Attachment 12.

Modeling and mesh generation using TrueGrid V2.3.0 software were executed on the following Hewlett-Packard (HP) 9000 Series workstations running operating system HP-UX 11.00:

Central Processing Unit (CPU) Name: Rosebud, Civilian Radioactive Waste Management System Management (CRWMS M&O) Tag Number: 150689

CPU Name: Oliver, CRWMS M&O Tag Number: 150688

The suitability and adequacy of the generated mesh is based on visual inspection.

The commercially available mathematical code, Mathcad Version 13.0 (Software Tracking # 611161-13-00), hereinafter referred to as “Mathcad”, is used to linearly interpolate the material properties of Alloy 22 and 316 stainless steel with modified C and N₂ at the required temperatures of 150 °C (302°F) and 250 °C (482°F). The usage of Mathcad constitutes Level 2 software usage as defined in IT-PRO-0011 (Reference 2.1.3, Attachment 12). Mathcad version 13.0 is listed in the current Level 2 usage *Controlled Software Report*, as well as the *Repository Project Management Automation Plan* (Reference 2.1.4, Table 6-1). Mathcad version 13.0 was executed on an IBM Compatible PC running Windows XP Professional operating system. The accuracy of the equation solver was verified by hand calculation.

Note that a few simple hand calculations were performed.

4.3 STRESS ANALYSIS APPROACH

Three-dimensional quarter symmetry Finite Element Representations (FERs) of the EP was created using TrueGrid and dimensions of References 2.2.2 to 2.2.17, Assumption 3.2.4.

The FERs of the outer corrosion barrier (OCB) used to represent the TAD WP was created using TrueGrid and dimensions of References 2.2.18 to 2.2.20, Assumption 3.2.3. After the OCB model was completed the equivalent material density was calculated by using the model volume and quarter symmetry TAD WP mass. This will help to preserve the weight load effect of the WP on the EP without changing the mechanical properties of the OCB. The OCB model includes part of the top lid to help the structural stability of the model during the Finite Element Analysis.

The FER mesh is used in ANSYS to determine the structural response of the EP while loaded with the heaviest WP. The analysis is done for a lifting event of loaded EP and for a degraded EP rested on flat support while loaded with the heaviest WP.

The EP design stress intensity (SI) and contact bearing stress (Sb), results are reviewed to determine compliance with the requirements of the ASME Code Criteria compliance (Reference 2.2.21). The EP and OCB surface tensile stress results are reviewed to determine compliance with post-closure requirements criteria (Reference 2.2.32, Table 1, Items 08-05).

5 LIST OF ATTACHMENTS

Table 5-1 Table of Attachments

Attachment Number	Title	Pages
I	Attachment I – Compact Disk (CD 1 of 1)	N/A

Table 5-2 Attachment I Files

Name	Size (KB) *	Date	Time
D:\CD 1 of 1	<DIR>	8/03/07	08:42a
prop intep.xcmd	149	7/31/07	02:39a
D:\	<DIR>	8/03/07	08:42a
degraded_pallet_rt	<DIR>	7/29/07	10:33a
degraded_pallet_rt.inp	20,246	7/29/07	10:53a
degraded_pallet_rt.out	45,770	7/28/07	10:39a
degraded_pallet_rt.tg	35	7/29/07	10:44a
D:\CD 1 of 1	<DIR>	8/03/07	08:42a
degraded_pallet_150	<DIR>	7/31/07	01:17a
degraded_pallet_150.inp	19,206	7/29/07	10:51a
degraded_pallet_150.out	44,603	7/28/07	10:41a
degraded_pallet_150.tg	35	7/29/07	10:44a
D:\CD 1 of 1	<DIR>	8/03/07	08:42a
lift_pallet_rt	<DIR>	8/3/07	01:51a
lift_pallet_rt.inp	20,167	7/31/07	03:24p
lift_pallet_rt.out	47,771	7/31/07	03:34p
lift_pallet_rt.tg	33	7/31/07	03:25p
D:\CD 1 of 1	<DIR>	8/03/07	08:42a
lift_pallet_250	<DIR>	8/03/07	01:52a
lift_pallet_250.inp	21, 717	7/31/07	03:27p
lift_pallet_250.out	47, 020	7/31/07	03:27p
lift_pallet_250.tg	33	7/31/07	03:27p
D:\CD 1 of 1	<DIR>	8/03/07	08:42a
liftrtelist	<DIR>	8/03/07	02:02a
s1_lprtoebelist.inp	9	8/03/07	12:05a
s1_lprtpl6elist.inp	5	8/03/07	03:17a
sb_lprtoebelist.inp	24	8/03/07	12:05a
sb_lprtpl6elist.inp	9	8/03/07	11:20p
SINT_lprtpl6elist.inp	38	8/03/07	02:51a
D:\CD 1 of 1	<DIR>	8/03/07	08:42a]
lift250elist	<DIR>	8/03/07	02:27a
ocb_250elist.inp	8	8/02/07	01:39a
S1pl6_250elist.inp	6	8/02/07	10:56p
Sbpl6_250elist.inp	9	8/02/07	10:11a
SINTpl6-250elist.inp	27	8/02/07	10:30a

* Note - File size, Dates and Times may vary due to Operating System.

6 BODY OF CALCULATION

6.1 MATERIAL PROPERTIES

Material properties used in this calculation are listed in this section. Material properties at room-temperature 21°C (RT) (70°F), 150°C (302°F) and 250°C (482°F) are used to give bounding results. Since the required material properties are not listed in the cited sources, a linear interpolation technique is implemented to calculate material properties at the required temperatures.

Alloy 22 [ASME SB-575 UNS N06022]

Room temperature (RT) material properties and stresses.

- Density = 8690 kg/m^3 (0.314 lb/in^3)
(Reference 2.2.21, Section II, Part B, SB-575 Section 7.1; see Assumption 3.2.7)
- Modulus of elasticity = 206 GPa ($29,900.00\text{ ksi}$)
(Reference 2.2.21, Section II, Part D, Subpart 2, Table TM-4)
- Poisson's ratio = 0.278
(Reference 2.2.26, p. 143; see Assumption 3.2.1 and Assumption 3.2.7)
- Yield strength = 310 MPa (45.00 ksi)
(Reference 2.2.21, Section II, Part D, Subpart 1, Table Y-1)
- Tensile strength = 689 MPa (100.00 ksi)
(Reference 2.2.21, Section II, Part D, Subpart 1, Table U)

Linear interpolation at 150°C (302°F) and 250°C (482°F):

Material properties for different temperature values are listed in Reference 2.2.21. Material properties for temperature values not listed on Reference 2.2.21 can be interpolated by using the point-slope equation.

$$(p - p_1) = m(t - t_1) \quad \text{Equation 5.1}$$

$$m = \frac{p_2 - p_1}{t_2 - t_1} \quad \text{Equation 5.2}$$

where

- p material property needed at a required temperature t
- p_1 material property at temperature t_1
- p_2 material property at temperature t_2
- m slope of a straight line

Using Equations 5.1, 5.2, and Reference 2.2.21, Section II, Part D, Table TM-4 – Material Group G – See Attachment I – prop interp.xmcd

- Modulus of elasticity = 198 *GPa* (28,690.00 *ksi*) (at 150°C (302°F))
- Modulus of elasticity = 193 *GPa* (28,060.00 *ksi*) (at 250°C (482°F))

Using Equations 5.1 ,5.2 , and Reference 2.2.21, Section II, Part D, Subpart 1, Table Y-1 – See Attachment I – prop interp.xmcd

- Yield strength = 254 *MPa* (36.85 *ksi*) (at 150°C (302°F))
- Yield strength = 225 *MPa* (32.62 *ksi*) (at 250°C (482°F))

Using Equations 5.1 ,5.2 , and Reference 2.2.21, Section II, Part D, Subpart 1, Table U – See Attachment I – prop interp.xmcd

- Tensile strength = 679 *MPa* (98.44 *ksi*) (at 150°C (302°F))
- Tensile strength = 644 *MPa* (93.40 *ksi*) (at 250°C (482°F))

316 SS with modified C and N₂ [ASME SA-240 UNS S31600]

Room temperature (RT) material properties and stress

- Density = 7980 *kg/m³* (0.2883 *lb/in³*)
(Reference 2.2.23, Table XI.1, p. 7; see Assumption 3.2.7)
- Poisson's Ratio = 0.30
(Reference 2.2.26, Figure 15, p. 755; see Assumption 3.2.7)
- Modulus of Elasticity = 195 *GPa* (28,300.00 *ksi*)
(Reference 2.2.21, Section II, Part D, Subpart 2, Table TM-1)
- Yield strength = 207 *MPa* (30.00 *ksi*)
(Reference 2.2.21, Section II, Part D, Subpart 1, Table Y-1)

Linear interpolation at 150°C (302°F) and 250°C (482°F):

Using Equations 5.1 ,5.2 , and Reference 2.2.21, Section II, Part D, Table TM-1 – Material Group G – See Attachment I – prop interp.xmcd

- Modulus of elasticity = 186 *GPa* (26,900.00 *ksi*) (at 150°C (302°F))
- Modulus of elasticity = 179 *GPa* (25,910.00 *ksi*) (at 250°C (482°F))

Using Equations 5.1, 5.2, and Reference 2.2.21, Section II, Part D, Subpart 1 Table Y-1 – See Attachment I – prop interp.xmcd

- Yield strength = 161 *MPa* (23.37 *ksi*) (at 150°C (302°F))
- Yield strength = 140 *MPa* (20.31 *ksi*) (at 250°C (482°F))

6.2 PRE-CLOSURE LIFT ACCELERATION

The lift acceleration used in this calculation is 10.81 m/s^2 . A lifting acceleration of 1 m/s^2 is added to gravitational acceleration (9.81 m/s^2) (see Assumption 3.2.6).

6.3 POST-CLOSURE THICKNESS REDUCTION

For the post-closure degraded EP static analysis, thickness reduction of 2.56 mm (Reference 2.2.24, and Assumption 3.2.5) is applied on the external surfaces of the structural components of the EP.

6.4 FINITE ELEMENT REPRESENTATIONS

Three-dimensional quarter-symmetry Finite Element Representation (FER) model of the EP is created in TrueGrid for this analysis. The model of the EP is created with solid brick elements using dimensions provided in References 2.2.2 through 2.2.17 and Assumption 3.2.4. A quarter symmetry representation of the mesh used in ANSYS is shown in Figures 6-1 to 6-3. The TAD WP dimensions and mass (Reference 2.2.18 to 2.2.20 and Assumption 3.1.1) is represented by a quarter symmetry model of the OCB. The total mass of the TAD WP, $73,509 \text{ kg}$ ($162,055 \text{ lbm}$) (Reference 2.2.27, Table 7-1 ; see Assumptions 3.1.1) is divided into four and the result mass is used as OCB model mass in the Finite Element Analysis. In order to simulate the weight of the TAD WP, the density of the OCB model is back calculated using quarter mass of the TAD WP and OCB model volume (see Assumption 3.2.3). The static friction coefficient between contact surfaces used in the analysis is based on Assumption 3.2.2.

For both lift and degraded analysis cases all the structural components of the EP were modeled except for simple round-offs on some components (see Assumption 3.2.4) and used in the Finite Element Analysis.

For the lift analysis the EP quarter symmetry model was constrained at the symmetry boundary planes, and make contact with the support at Plate 9 (Reference 2.2.14), part of the lifting feature is modeled only for the purpose of constraining the EP at Plate 9 by contact and no analysis was done on the support structural component which is part of the *Transport and Emplacement Vehicle*. The OCB model is also constrained at the symmetry planes. The lift analysis was performed for material properties at room temperature 21°C (70°F) and at 250°C (482°F). The peak surface temperature of the OCB of the TAD WP is bounded by 250°C (Reference 2.2.30, Table 50).

The degraded EP analysis was performed by constraining the structural components of the EP model at the symmetry boundary planes, and at the bottom support, Plate 1 (Reference 2.2.6). The thickness reduction due to corrosion and the temperature at which the material properties should be considered is given on the *IED Emplacement Pallet* (Reference 2.2.24). The post-closure degraded analysis was performed by using material properties at room temperature 21°C (70°F) and at 150°C (302°F) (Reference 2.2.32, Item 08-03).

The ANSYS runs for all temperature cases were performed with two load steps, the first load step

brings the OCB into contact with the EP, Plate 6 (Reference 2.2.11), this process mitigates the problem of convergence during the analysis by making a smooth contact process between the contact structural components. The second load step starts after the first load step converges, the inertia load of the OCB is applied at the second load step. For the lift analysis inertia load, 10.81 m/s^2 (see Assumption 3.2.6) acceleration is used. For the degraded analysis the gravitational acceleration (9.81 m/s^2) is used. The outputs of the second load step (last load step) are used for the required analyses.

Figure 6-1 shows the FERs model of the EP and the WP OCB used for the lift and degraded analysis, at the required temperatures (RT , 150°C and 250°C). Figure 6-2 shows the EP model for lift analysis at RT and 250°C . Figure 6-3 shows the EP model used for degraded analysis at RT and 150°C . The OCB model is left out in Figures 6-2 and 6-3 to show a magnified view of the EP model. Figure 6-4 shows an isometric view of the EP model. The Mesh density of the model for all the runs is the same; the difference is that the material property used at each required temperature and the constrained structural components for the required analysis type (lift or degraded). For the postclosure degraded analysis a thickness reduction of 2.56 mm is applied on the surfaces of Alloy 22 structural components of the EP. Material properties at the required temperature are listed Section 6.1.

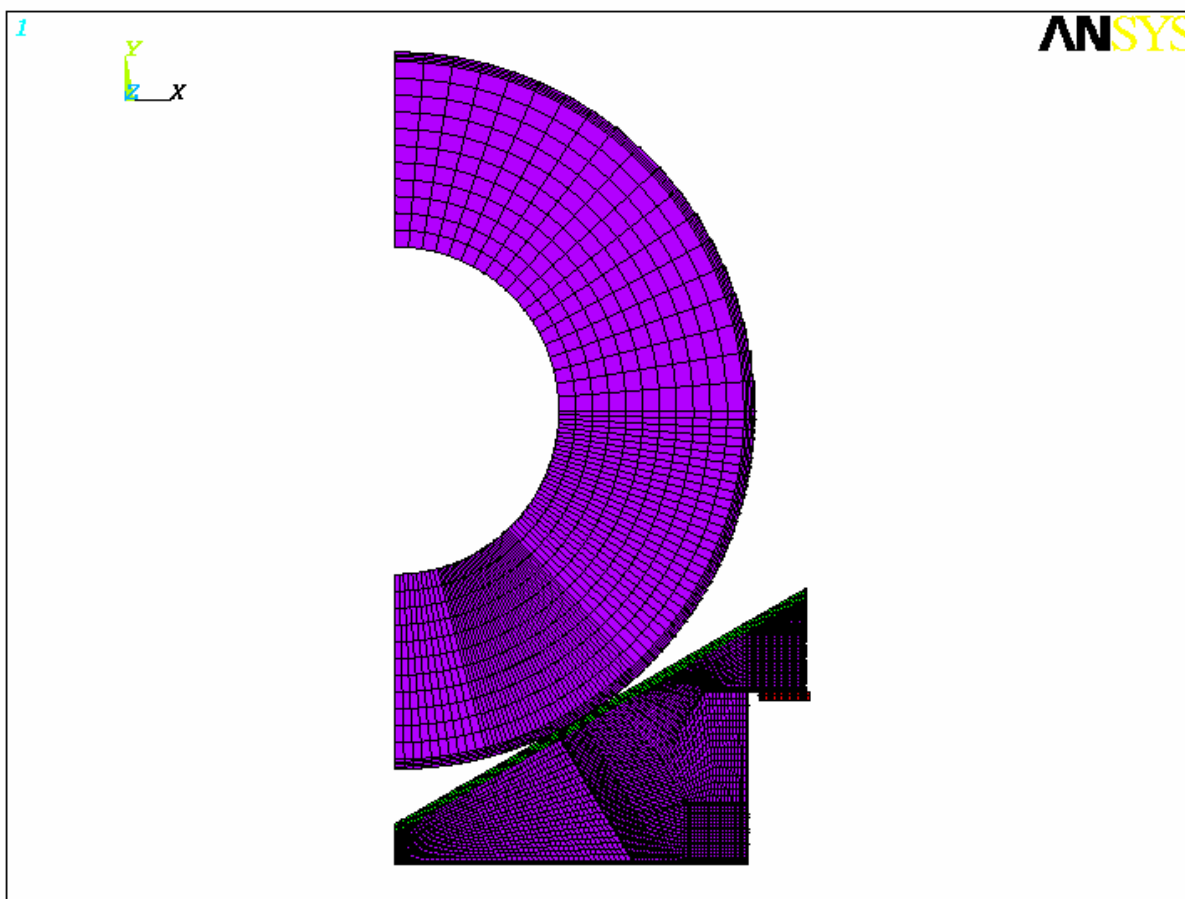


Figure 6-1 EP and OCB Finite Element Model used for the Analysis

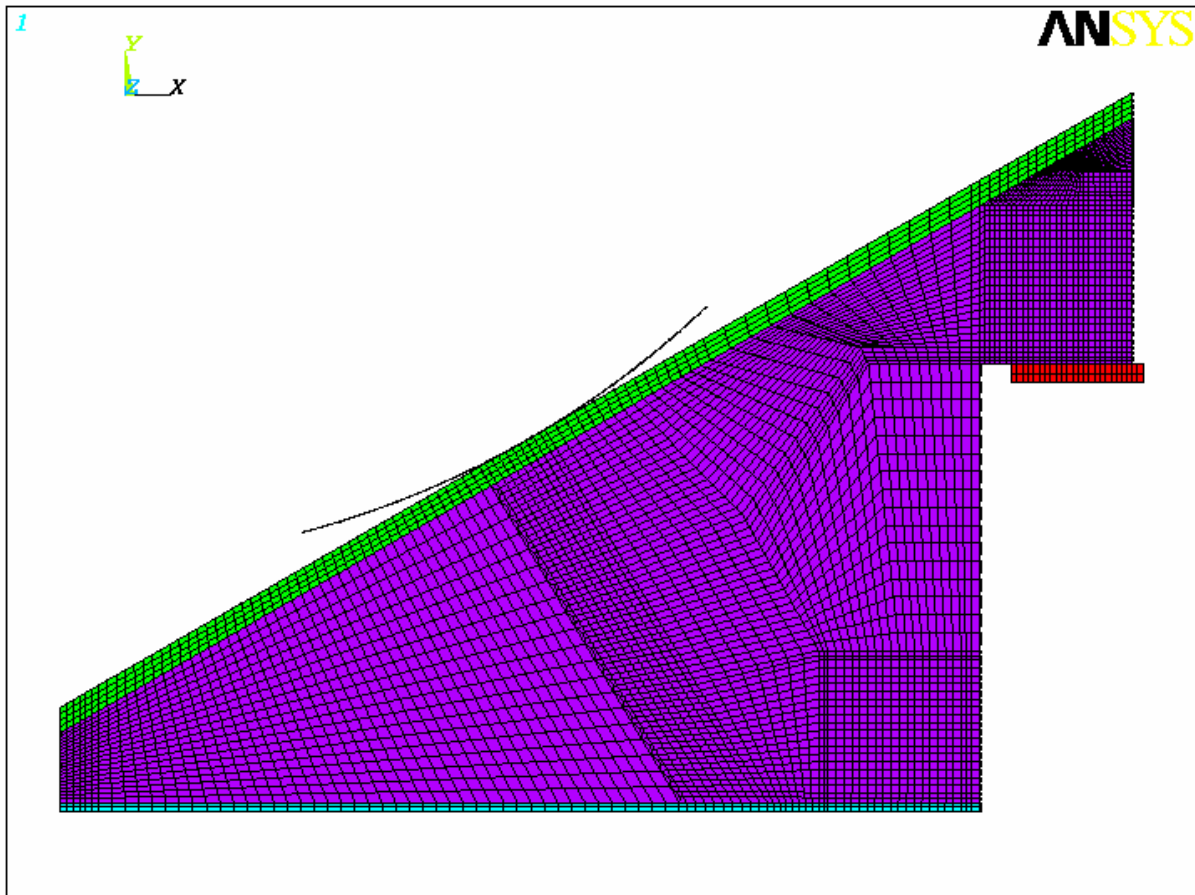


Figure 6-2 EP Model used for Lift Analysis at RT and 250 °C.

The tangent curve at the slope of Figure 6-2 is to show the contact surface curve between the WP OCB and the EP plate.

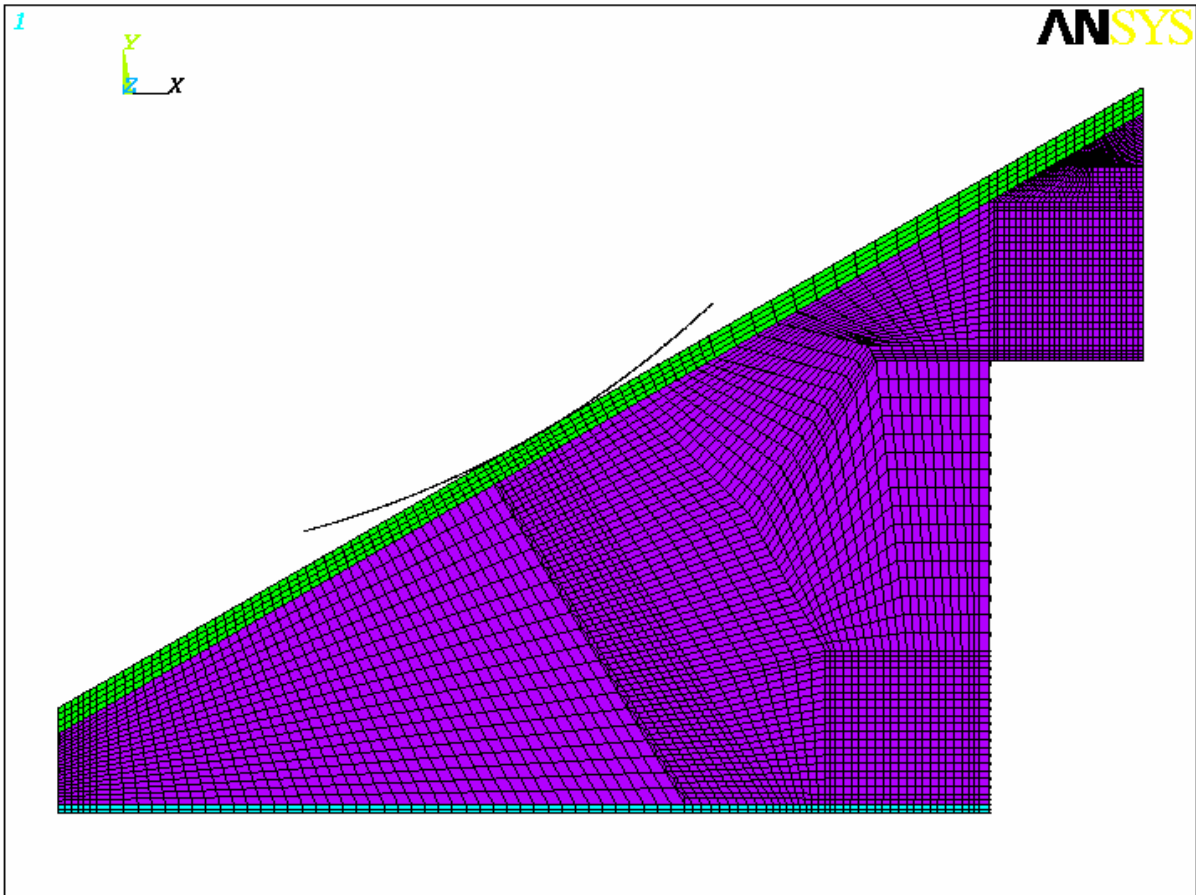


Figure 6-3 EP Model used for Degraded Static Analysis at RT and 150°C.

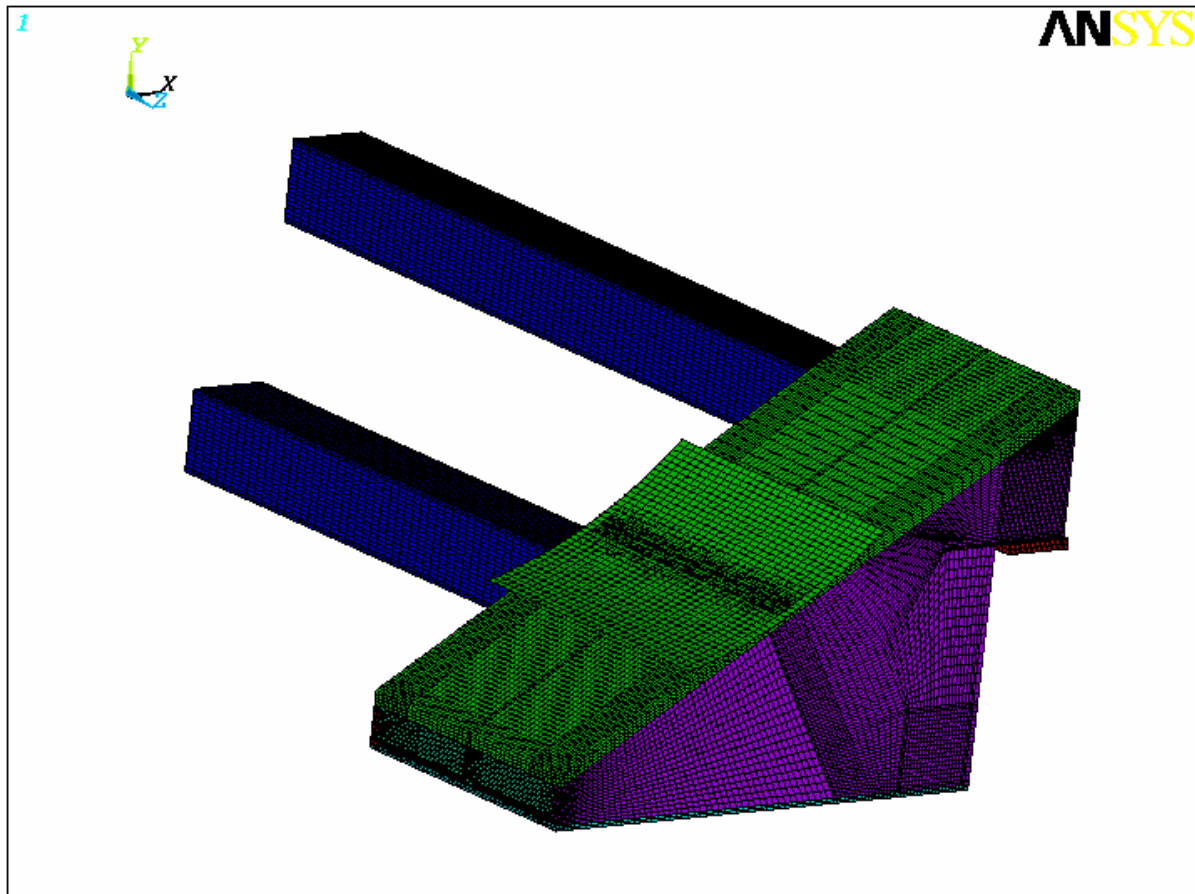


Figure 6-4 An Isometric View of Quarter Symmetry EP Model with Contact Surface.

7 RESULTS AND CONCLUSIONS

The following results obtained from ANSYS are reasonable compared to the inputs and are suitable for the intended use of this calculation.

7.1 ANALYSIS CRITERIA

The most appropriate criteria in the ASME B & PV Code for the subject evaluation is the rule for construction of component supports of Class 2 vessels designed to NC-3200. The design evaluation, for Plate-Type Supports per Reference 2.2.21, Section III, Division 1, NF-3000, Table NF-3131 (a)-1, Note (1) and Article NF-3142 is elastic analysis based on maximum stress intensity (SI), with allowable limits contained in NF-3220. The two basic normal condition limits are: the membrane stress intensity, Pm must be less than the allowable design stress intensity value, Sm ; the primary membrane stress, Pm plus the primary bending stress, Pb excluding all secondary stress has to be less than $1.5*Sm$ (Reference 2.2.21, Section III, Division 1, NF-3221.1).

Pm in the EP plates would be the Element-Wall-Average (EWA) stress intensity, SI away from structural discontinuities. The sum of the primary membrane and primary bending, $(Pm+Pb)$, would be the surface SI in the plates away from structural discontinuities. Structural discontinuities are corners, and change in thickness. Location of stress singularities should be either ignored or SI values extrapolated there into. These are locations at the nodal constraints.

The allowable design stress intensity, Sm values are in Section II of the ASME B& PV Code and reduce with temperature. Since elastic analysis is being conducted, and the weight primary stresses will in theory be constant even with reduced Modulus of Elasticity.

The average bearing stress, (Sb) for resistance to crushing under the maximum load experienced as a result of design loading shall be limited to yield stress, (Sy) at temperature (Reference 2.2.21, Section III, Division 1, NF-3223.1). The bearing stress is not stress intensity; the bearing stress is the compressive stress component normal to the contact surfaces. Since the contact between the WP OCB and Plate 6 (Reference 2.2.11) of the EP is at 30° from the horizontal axis (X-axis), the normal bearing stress is the sum of the normal component of the normal stress in the X and Y-axes. The bearing stress was calculated by selecting a row of contact elements at the surface of the contact structure. The average bearing stress, (Sb) is plotted using ANSYS for the contact surfaces of the OCB and the EP.

The mathematical equation used to compute each bearing stress for the selected contact elements is given in Equation (7-1);

$$Sb = \sin(\theta)*Sx + \cos(\theta)*Sy \quad \text{Equation (7-1)}$$

Where:

$$\begin{aligned} Sb &= 0.5*Sx + 0.866*Sy \\ \theta &= 30^\circ \text{ (for Plate 6 and the WP OCB)} \\ Sx &\text{ is normal stress in the X-axis} \end{aligned}$$



S_y is normal stress in the Y-axis
 $0.5 = \sin(30)$ and $0.866 = \cos(30)$

na
 08/16/07

The maximum tensile stress imposed on the external surfaces of the structural elements of Alloy 22 for the EP and the WP OCB must be less than 257 MPa (the approximate stress corrosion cracking threshold of Alloy 22) (Reference 2.2.32 Table 1, Item 08-05). Compliance with this requirement is checked by locating surface elements with maximum tensile stress and plotting the maximum principal stress SI , for both the EP and the OCB. From mechanics of materials, of the three principal stresses, the first principal stress is the most positive and the third principal stress is the most negative stress.

The basis for establishing the allowable design stress intensity SI , values is given in Reference 2.2.21, Section II, Part D, Appendix 1. The allowable design stress intensity values for Alloy 22 are also given in Reference 2.2.21, N-621, Table 2 and are used for this calculation.

The allowable design stress intensity S_m values are listed below in Table 6-1 (Reference 2.2.21, Code Cases, Nuclear, N-621, Table 2);

Table 7-1 ASME Allowable Design Stress Intensity Values

7-1 na
 08/10/07

Temperature Not Exceeding,		ASME Design Stress Intensity		Design Stress Intensity used	
(°F)	(°C) [1]	S_m (ksi)	S_m (MPa) [2]	$1.5 \cdot S_m$ (ksi)	$1.5 \cdot S_m$ (MPa)
-20 to 100	-29 to 38	30	207	45	310
300	149	30	207	45	310
400	204.44	30	207	45	310
500	260	29	200	43.5	300

Note [1] $^{\circ}\text{C} = (0.556 \cdot ^{\circ}\text{F} - 17.78)$

[2] $1 \text{ ksi} = 6.895 \text{ MPa}$

The maximum stress intensity, SI is the magnitude of the largest value of the difference between any of the three principal stresses.

7.2 CONCLUSIONS

Table 7-2 shows the summarized results of the average maximum bearing stress (S_b), the average maximum stress intensity (SI) and the maximum principal stress (SI) for the EP lift analysis while loaded with the heaviest WP (TAD). Plate 6 of the EP, which supports the WP, has the highest average maximum stress intensity. Tube 3, which is welded to Plate 6 serves as a support where the contacts occur between the WP and Plate 6 of the EP. The lift support makes contact with the EP on Plate 9, which is welded at the bottom of Tube 1. Reporting the stress intensity of the OCB is not in the scope of this document.

Table 7-2 Stress Results Table for EP Lift Analysis While Loaded With TAD WP

Temp.	Part Name	Average Maximum Bearing Stress, S_b (MPa) (Compressive)	Average Maximum Stress intensity SI (MPa)	Maximum Principal Stress $S1$ (MPa) (Tensile)
21 °C (70°F) RT	EP-Plate 6	-286 (Fig. 7-1)	276 (Fig. 7-2)	23.9 (Fig. 7-3)
	EP-Plate 9	-109 (Fig. 7-5)	205 (Fig. 7-4)	18.7 (Fig. 7-6)
	EP-Tube 3	-	156	51.6
	WP OCB	-210 (Fig. 7-7)	-	56.8 (Fig. 7-8)
250 °C (482°F)	EP-Plate 6	-286 (Fig. 7-9)	274 (Fig. 7-10)	28.2 (Fig. 7-11)
	EP-Plate 9	-110 (Fig. 7-12)	206 (Fig. 7-13a)	16.4 (Fig. 7-13b)
	EP-Tube 3	-	156	51.6
	WP OCB	-210 (Fig. 7-15)	-	56.8 (Fig. 7-14)

The result outputs in Table 7-2 obtained from ANSYS show that the average maximum stress intensities of the listed structural components of the EP satisfy the allowable design limit stress intensities given in Table 7-1, which is 310 MPa for RT and 300 MPa for 250 °C. Table 7-2 also shows that the maximum tensile stress on the surfaces of the structural elements of the components of the EP and the WP OCB is under 257 MPa, and satisfies the requirements of Reference 2.2.32, Table 1, Item 08-05. The stress results of Tube 3 are not included in the figure plots.

Table 7-3 summarizes the results of the average maximum bearing stress (S_b), the average maximum stress intensity (SI) and the maximum principal stress (SI) for the degraded EP while loaded with the heaviest WP (TAD) after 10,000 years and the WP OCB. Plate 6 of the EP which supports the WP has the highest average maximum stress intensity. Tube 3, which is welded to Plate 6 and serves as a support where the contacts occur between the WP and Plate 6 of the EP. Figures 7-17 and 7-21 maximum stress intensity plots shows that the stress intensity on the EP is under the allowable design stress intensity limits. The plots are also complied with the post-closure tensile stress requirement.

Table 7-3 Stress Results Table for Degraded EP Static Analysis While Loaded With TAD WP

Temp.	Part Name	Average Bearing Stress, S_b (MPa) (Compressive)	Average Maximum Stress Intensity S_I (MPa)	Maximum Principal Stress S_1 (MPa) (Tensile)
21 °C (70°F) RT	EP-Plate 6	-163 (Fig. 7-17)	204 (Fig. 7-16)	55.1 (Fig.7-18)
	EP-Plate1	-24.3	28	17
	EP-Tube 3	-	121	34.7
	WP OCB	-121 (Fig. 7-19)	-	32.4 (Fig 7-20)
150 °C (302°F)	EP-Plate 6	-163 (Fig. 7-22)	201 (Fig. 7-21)	54.6 (Fig. 7-24)
	EP-Plate 1	-24.3 (Fig. 7-26)	27.9	17 (Fig. 7-25)
	EP-Tube 3	-	121	34.7
	WP OCB	-152 (Fig.7-28)	-	24.7 (Fig. 7-27)

The result outputs in Table 7-3 obtained from ANSYS show that the average maximum stress intensities of the listed structural components of the EP satisfy the design limit stress intensities given in Table 7-1, which is 310 MPa for RT and 310 MPa for 150 °C. Table 7-2 also shows that the maximum tensile stress on the surfaces of the structural elements of the components of the EP and the WP OCB is under 257 MPa, and satisfies the requirements of Reference 2.2.32, Table1, Item 08-05. Plots of Plate 1, and Tube 3 are not included in the document, since Figures 7-16 and 7-21 are under the allowable design stress intensity limit.

The output values are reasonable for the given inputs in this calculation. The uncertainties are taken into account by consistently using the most conservative approach; therefore the calculation yields a conservatively bounding set of results. The results are suitable for assessing the stress state of the emplacement pallet during these events.

7.3 EP LIFT ANALYSIS AT RT

Figure 7-1 shows the average bearing stress of the contact elements of Plate 6. Three rows of elements were selected across the top surface of the plate, for the list of selected elements see Section 5, Table 5-2, (Attachment I, D:\CD 1 of 1\liftrt_elist\sb_lprtpl6_elist.inp). The methodology used to calculate the bearing stress is explained Section 7.1. Magnitude of the average maximum bearing stress (S_b) is 286 MPa, which is less than the allowable design stress intensity limit (S_m), 310 MPa.

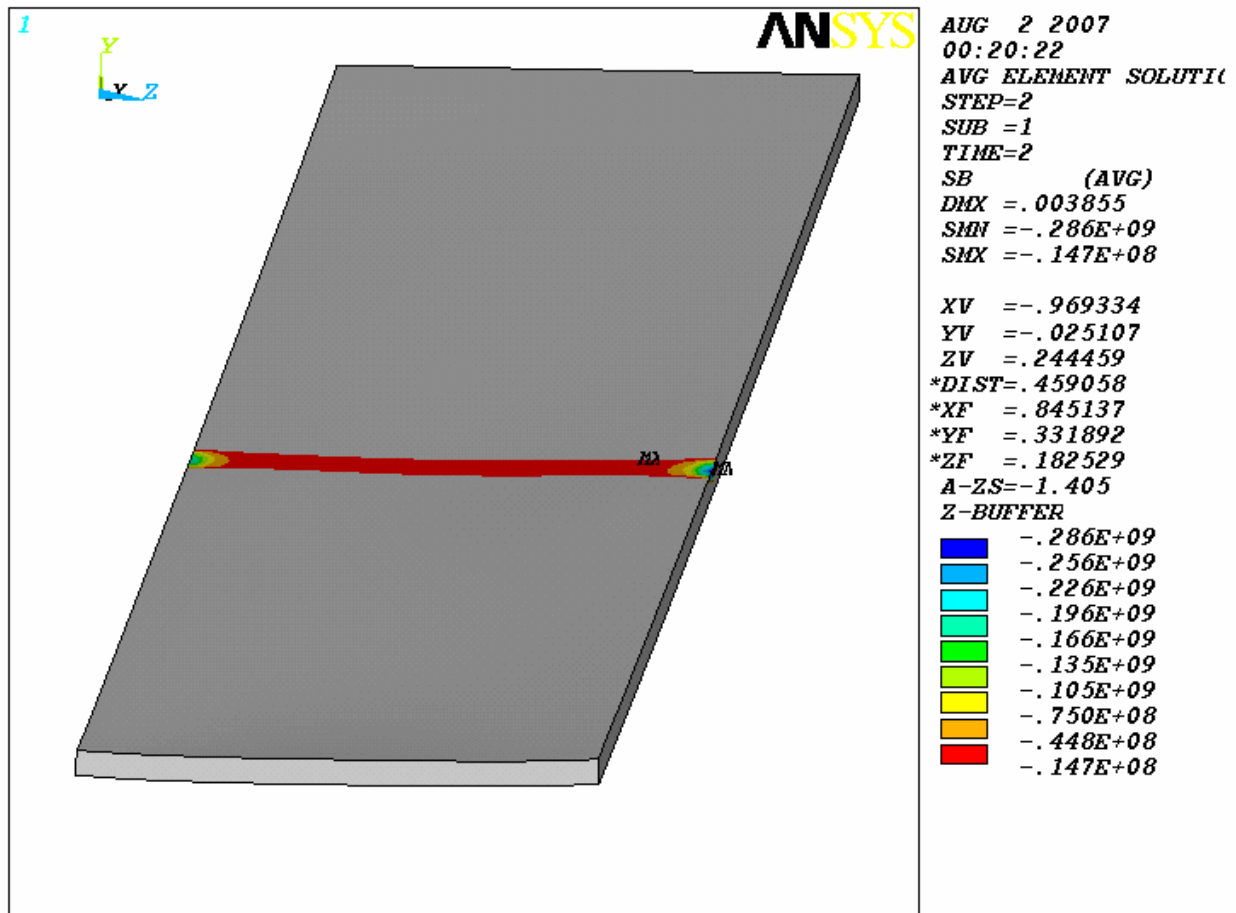


Figure 7-1 Average Bearing Stress S_b [Pa] of Plate 6 for EP Lift Analysis at RT

Figure 7-2 shows the average maximum stress intensity of Plate 6. The list of structural elements selected to compute the average stress intensity are given in Section 5, Table 5-2, (Attachment I, D:\CD 1of 1\liftrt_elist\SINT_lprtpl6_elist.inp). Corner elements with high-localized stress are excluded from the plot. The plot shows that the average maximum stress intensity, (SI) 276 MPa , is less than the allowable design stress intensity limit (Sm), 310 MPa .

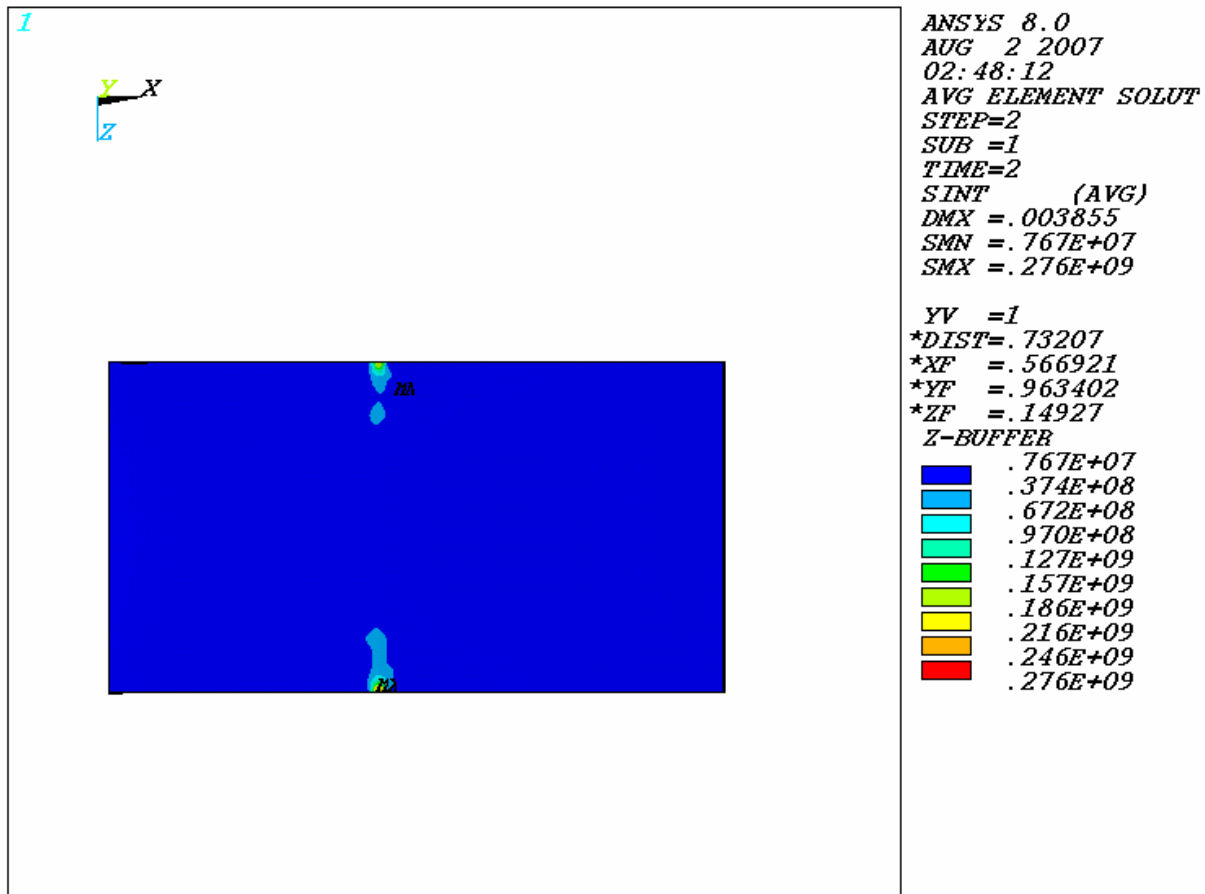


Figure 7-2 Average Maximum Stress Intensity, SI [Pa] of Plate 6 for EP Lift Analysis at RT

Figure 7-3 shows the plot of the average maximum tensile stress on the surface elements of Plate 6. For the list of selected elements to compute the tensile stress see Section 5, Table 5-2, (Attachment I, D:\CD 1 of 1\liftrt_elist\s1_lprtpl6_elist.inp). The plot result shows that the tensile stress acting on the surface of Plate 6 of the EP, 23.9 MPa is less than the bounding limit of 257 MPa.

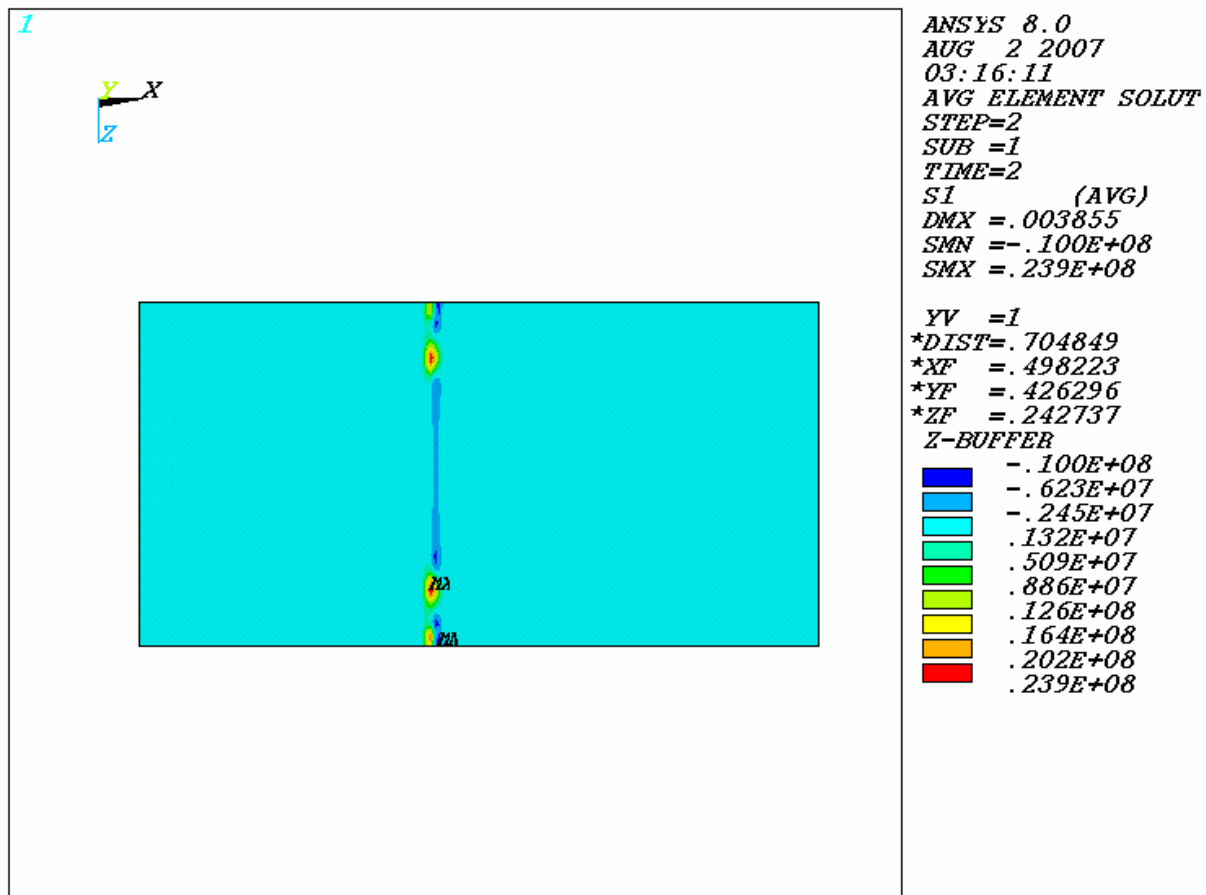


Figure 7-3 Average Maximum Tensile Stress, S1 [Pa] of Plate 6 for EP Lift Analysis at RT

Figure 7-4 shows the maximum stress intensity of Plate 9, where the EP is constrained for lift. The corner elements with high-localized stress due structural discontinuity are excluded from the plot. The plot shows that the maximum stress intensity, (SI) 205 MPa , is less than the allowable design stress intensity limit (Sm), 310 MPa .

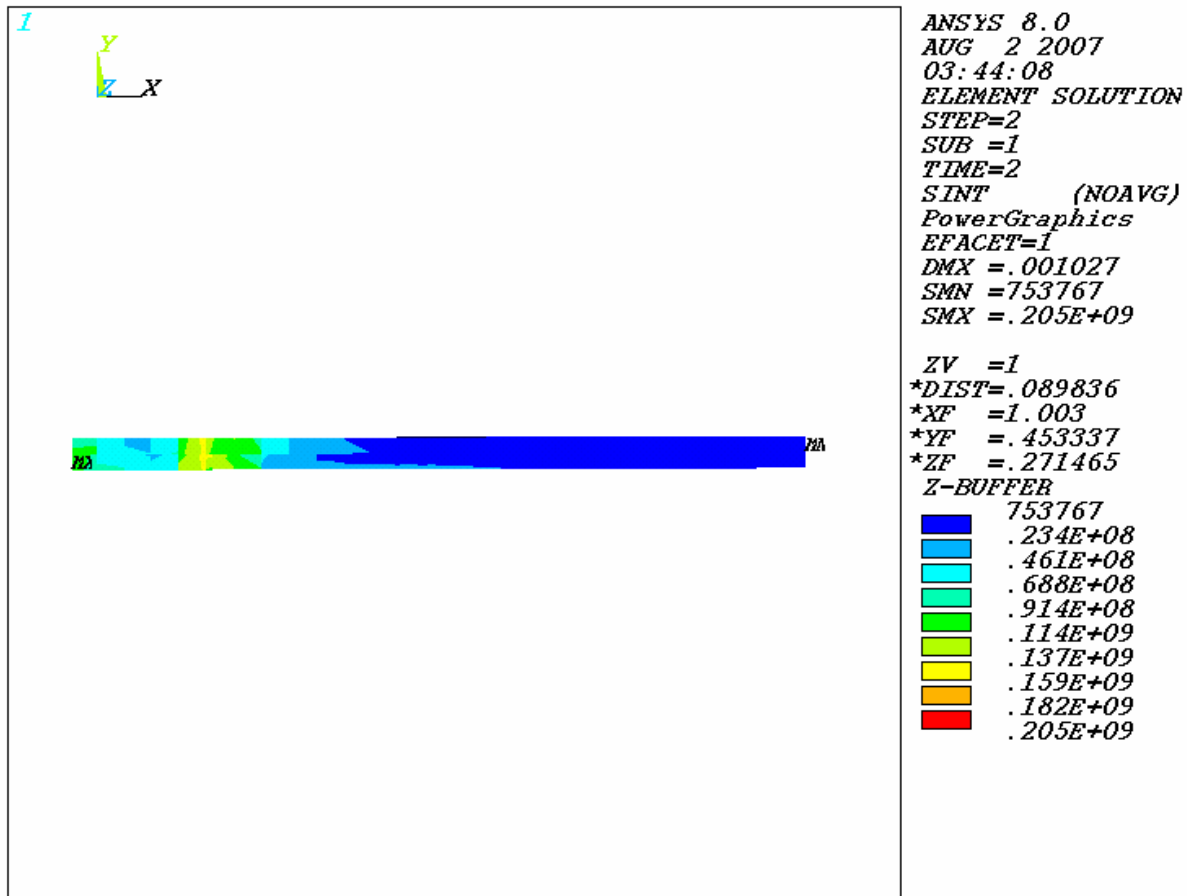


Figure 7-4 Maximum Stress Intensity SI [Pa] of Plate 9 for EP Lift Analysis at RT.

Figure 7-5 shows the bearing stress of the contact elements of Plate 9. Structural elements under the

contact surface are used. The methodology used to calculate the bearing stress is explained Section 7.1. Magnitude of the maximum bearing stress (S_b) is 109 MPa, which is less than the allowable design stress intensity limit (S_m), 310 MPa.

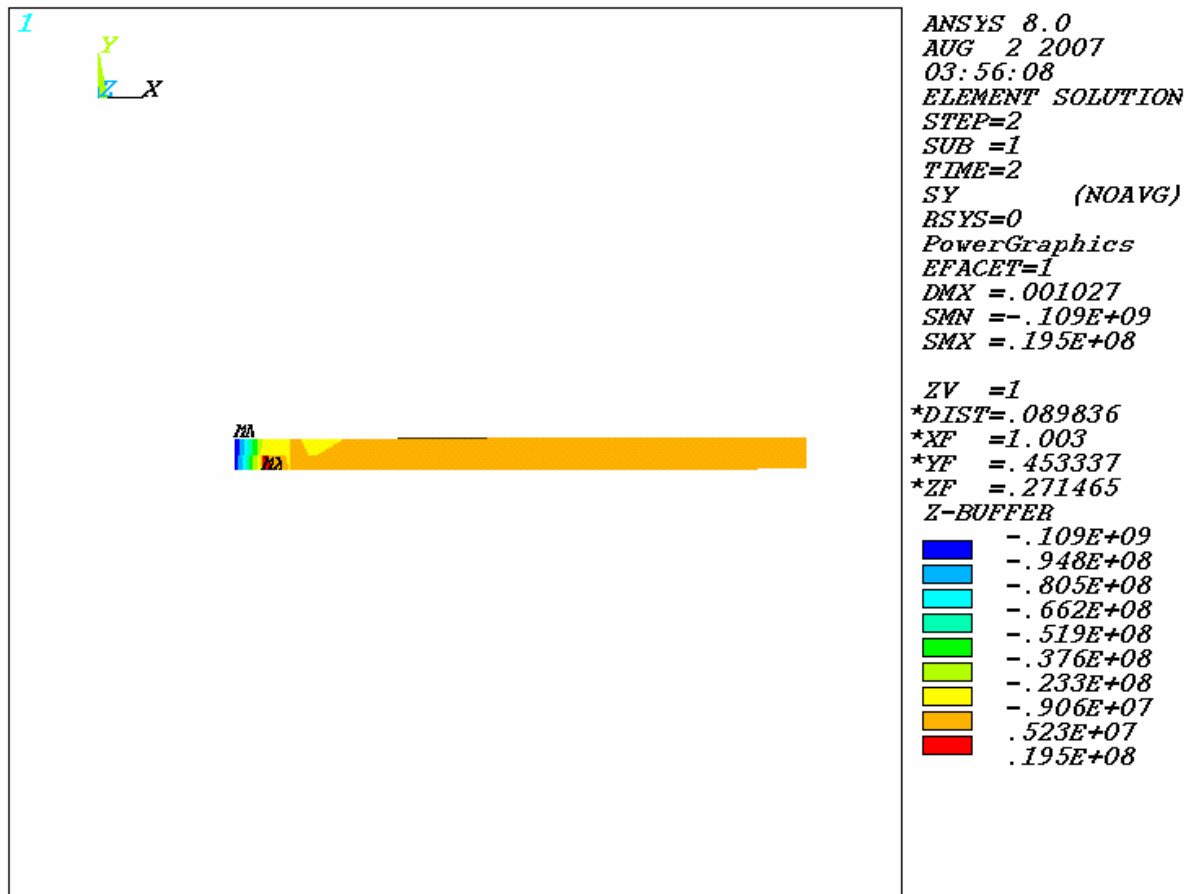


Figure 7-5 Bearing Stress S_b [Pa] of Plate 9 for EP Lift Analysis at RT

Figure 7-6 shows the plot of the tensile stress on the surface elements of Plate 9. The plot result shows that the tensile stress acting on the surface of Plate 9 of the EP, 18.7 MPa is less than the bounding limit of 257 MPa .

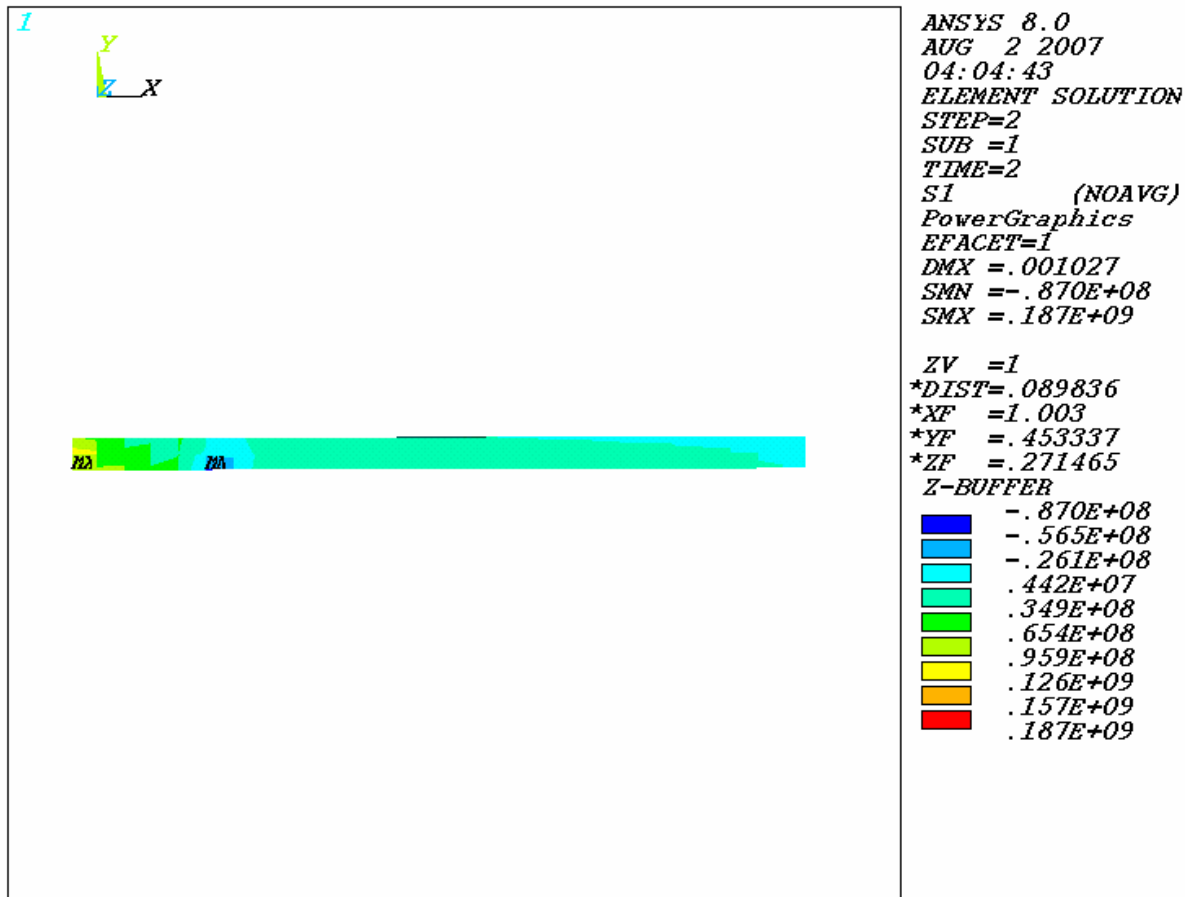


Figure 7-6 Maximum Tensile Stress, $S1$ [Pa] of Plate 9 for EP Lift Analysis at RT

Figure 7-7 shows the average bearing stress of the contact elements of WP OCB. The rows of elements selected across the contact surface of the WP OCB are given in Section 5, Table 5-2, (Attachment I, D:\CD1 of 1\lifrtr_elist\sb_lprtoch_elist.inp). The methodology used to calculate the bearing stress is explained Section 7.1. Magnitude of the average maximum bearing stress (S_b) is 210 MPa, which is less than the allowable design stress intensity limit (S_m), 310 MPa.

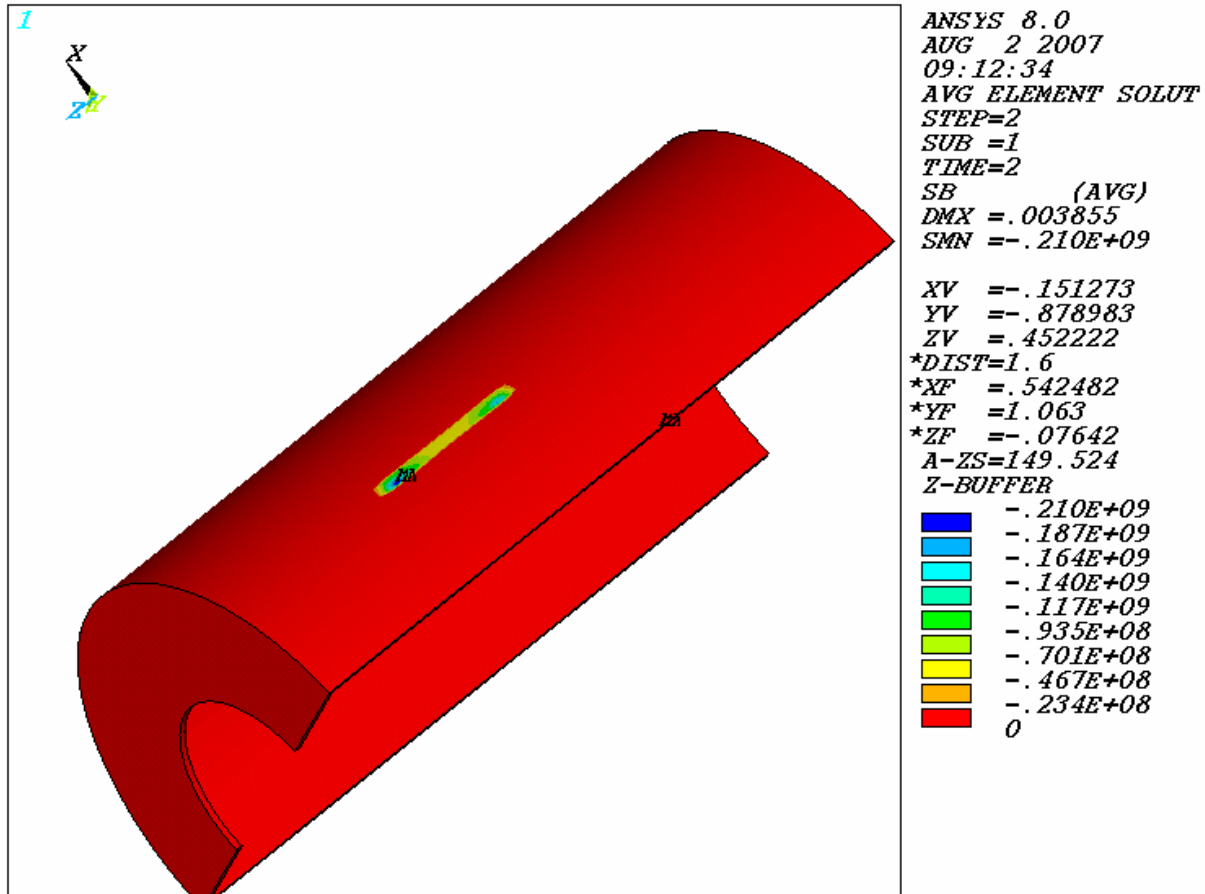


Figure 7-7 Average Bearing Stress S_b [Pa] of the OCB for EP Lift Analysis at RT

Figure 7-8 shows the plot of the tensile stress on the surface elements of the WP OCB. The list of selected elements to compute the tensile stress is given in Section 5, Table 5-2, (Attachment I, D:\CD 1 of 1\liftrt_elist\s1_lprtoch_elist.inp). The plot result shows that the average maximum tensile stress acting on the surface of WP OCB, 56.8 MPa is less than the bounding limit of 257 MPa.

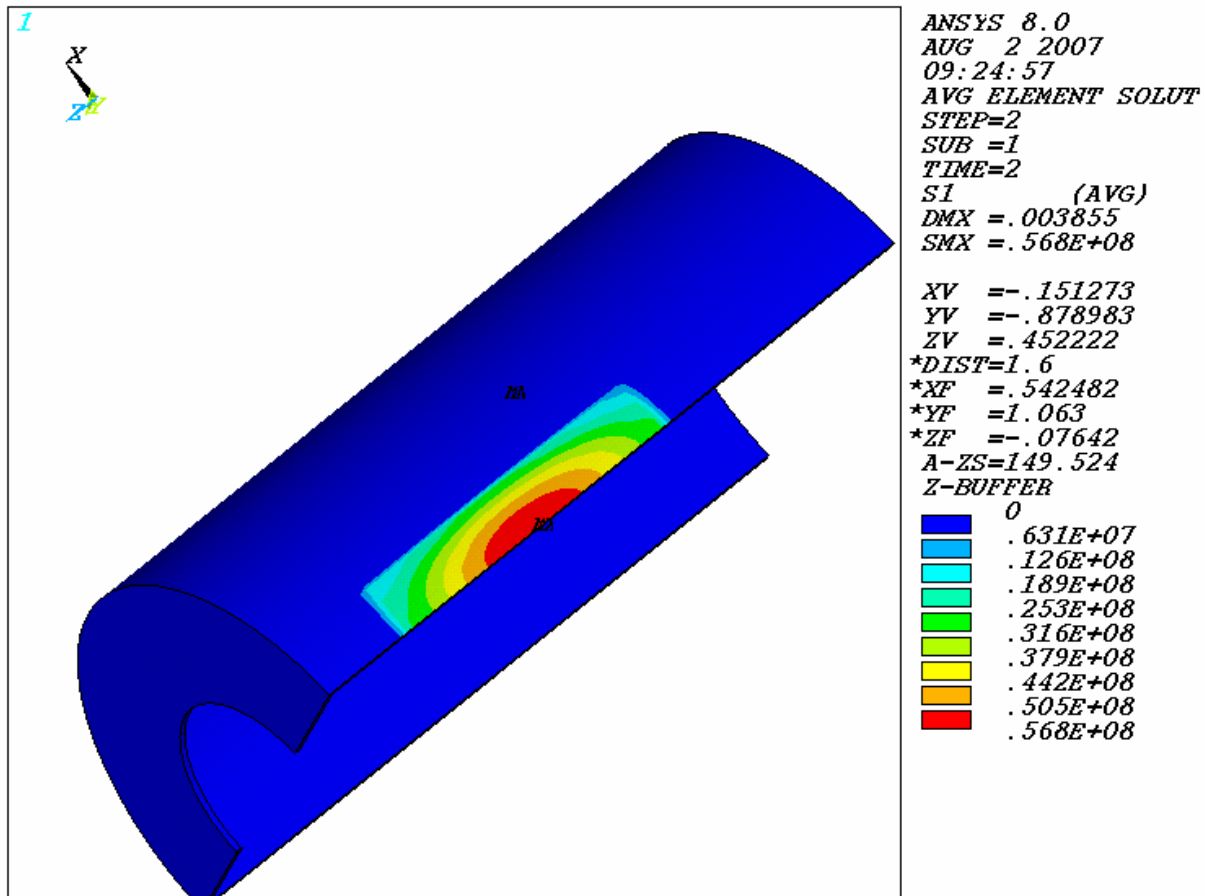


Figure 7-8 Average Maximum Tensile Stress, S1 [Pa] of the OCB for EP Lift Analysis at RT

7.4 EP LIFT ANALYSIS AT 250°C

Figure 7-9 shows the average bearing stress of the contact elements of Plate 6. Three rows of elements were selected across the top surface of the plate, for the list of selected elements see Section 5, Table 5-2, (Attachment I, D:\CD 1 of 1\lift250_elist\Sbpl6_250_elist.inp). The methodology used to calculate the bearing stress is explained Section 7.1. Magnitude of the average maximum bearing stress (S_b) is 286 MPa, which is less than the allowable design stress intensity limit (S_m), 310 MPa.

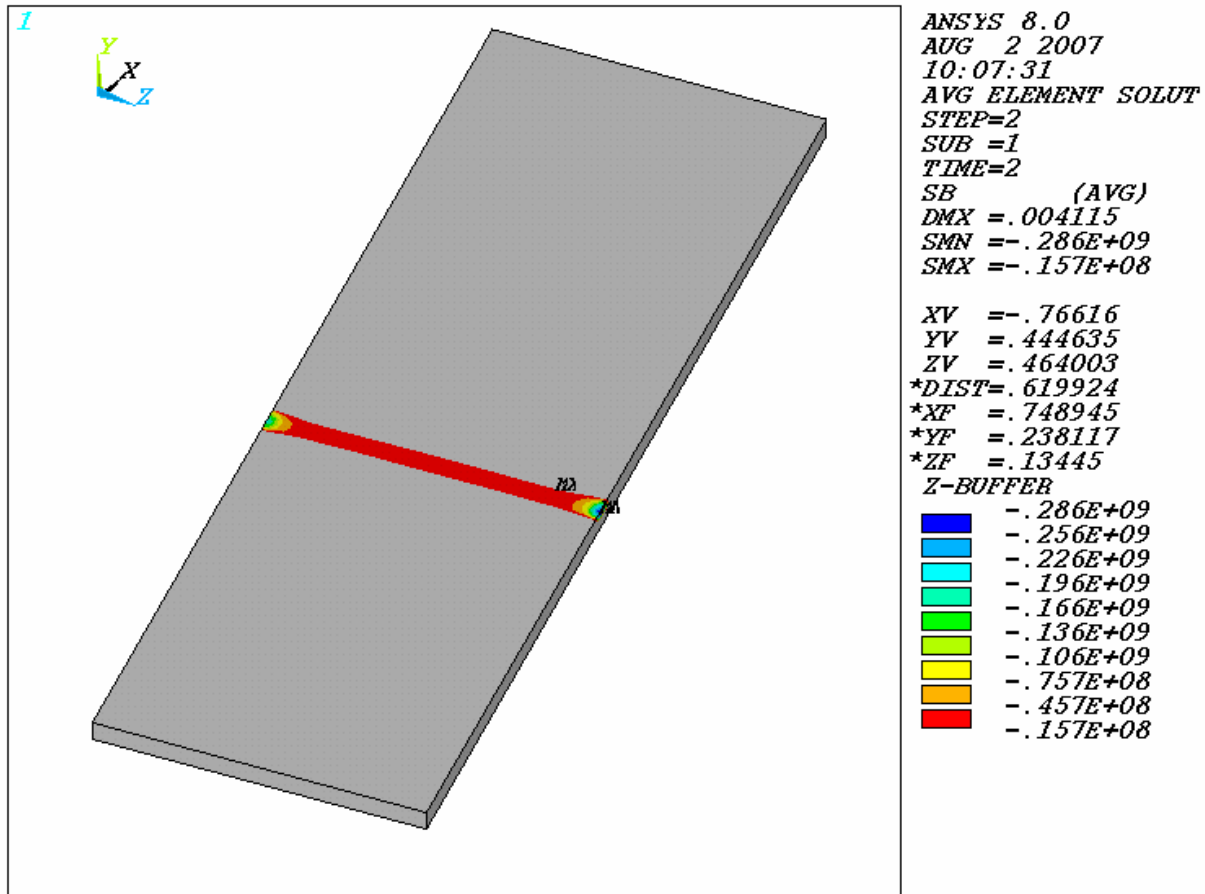


Figure 7-9 Average Bearing Stress S_b [Pa] of Plate 6 for EP Lift Analysis at 250°C

Figure 7-10 shows the average maximum stress intensity of Plate 6. The list of structural elements selected to compute the average stress intensity are given in Section 5, Table 5-2, (Attachment I, D:\CD 1 of 1\lift250_elist\SINTpl6_250elist.inp). Corner elements with high-localized stress are excluded from the plot. The plot shows that the average maximum stress intensity, (SI) 274 MPa , is less than the allowable design stress intensity limit (Sm), 310 MPa .

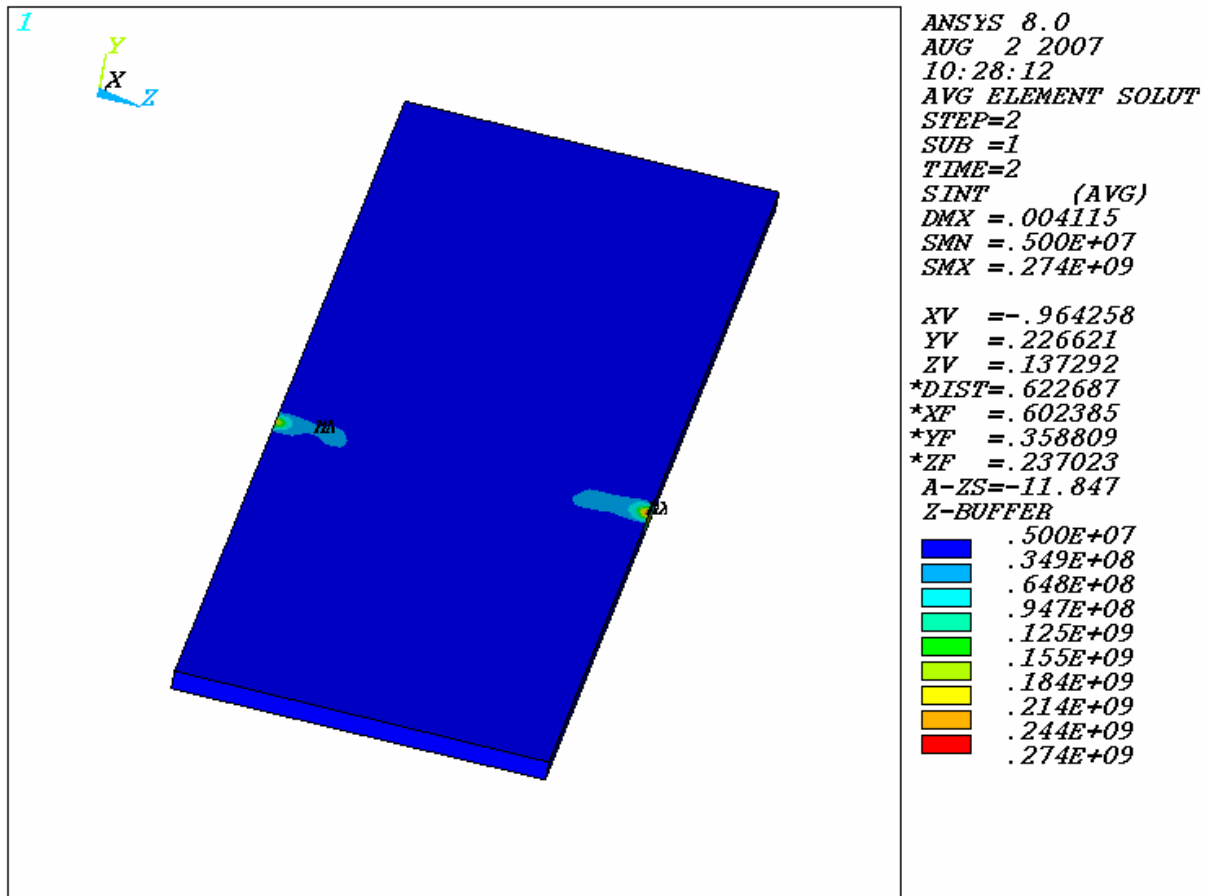


Figure 7-10 Average Stress Intensity SI [Pa] of Plate 6 for EP Lift Analysis at 250°C

Figure 7-11 shows the plot of the average maximum tensile stress on the surface elements of Plate 6. For the list of selected elements to compute the tensile stress see Section 5, Table 5-2, (Attachment I, D:\CD 1 of 1\lift250_elist\S1pl6_250elist.inp). The plot result shows that the tensile stress acting on the surface of Plate 6 of the EP, 28.2 MPa is less than the bounding limit of 257 MPa.

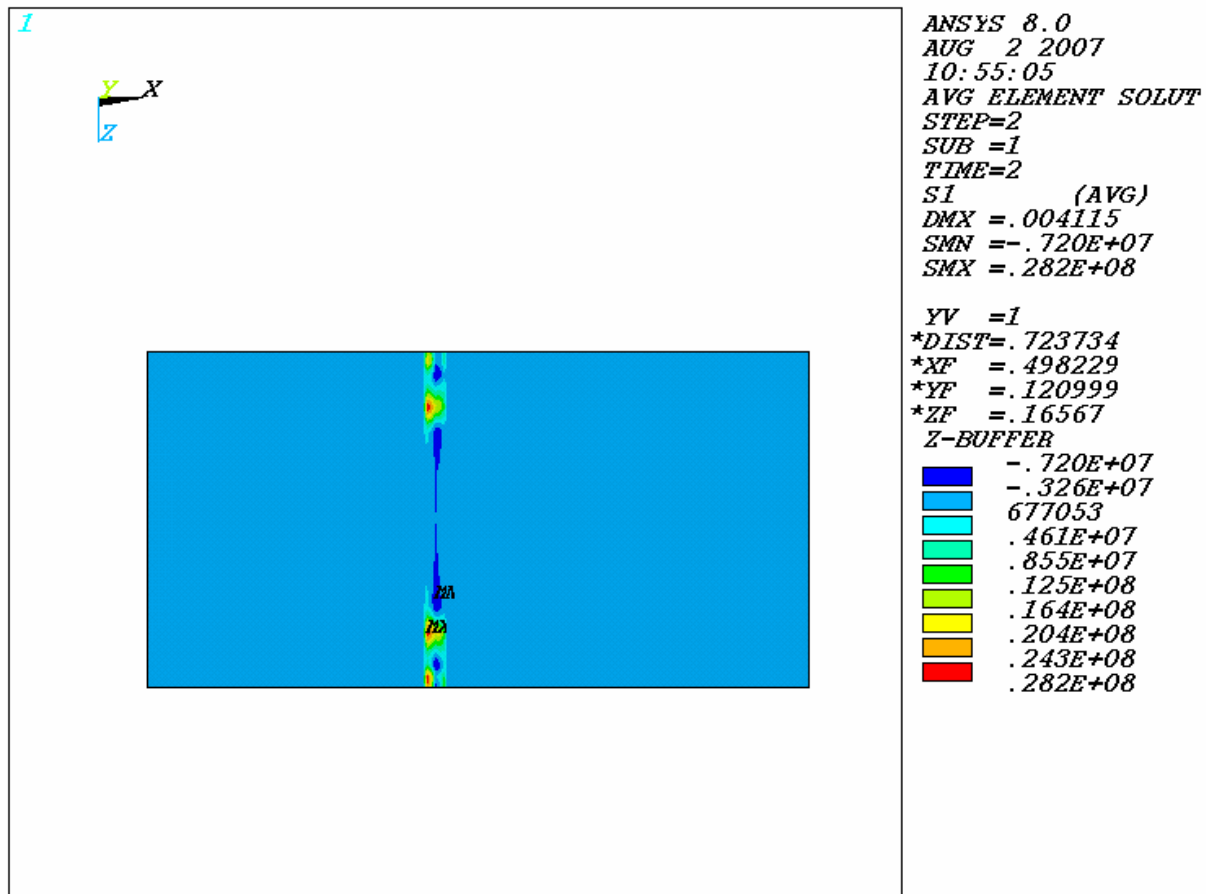


Figure 7-11 Average Maximum Tensile Stress, S1 [Pa] of Plate 6 for EP Lift Analysis at 250°C

Figure 7-12 shows the bearing stress of the contact elements of Plate 9. Structural elements under the contact surface are used. The methodology used to calculate the bearing stress is explained Section 7.1. Magnitude of the maximum bearing stress (S_b) is 110 MPa, which is less than the allowable design stress intensity limit (S_m), 310 MPa.

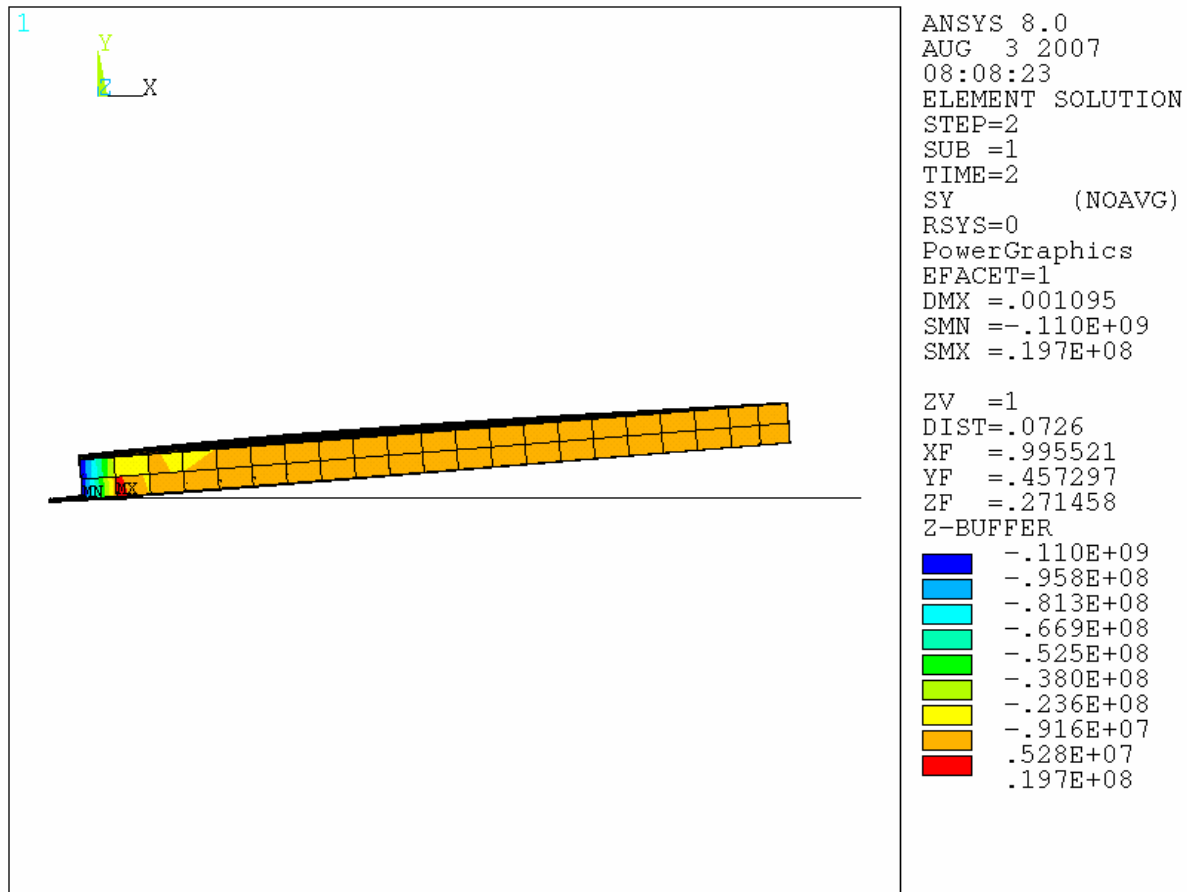


Figure 7-12 Bearing Stress S_b [Pa] of Plate 9 for EP Lift Analysis at 250 °C

Figure 7-13 shows the maximum stress intensity of Plate 9, where the EP is constrained for lift. The corner elements with high-localized stress due structural discontinuity are excluded from the plot. The plot shows that the maximum stress intensity, (SI) 206 MPa , is less than the allowable design stress intensity limit (Sm), 310 MPa .

The tensile stress on the surface elements of Plate 9 is 16.4 MPa is less than the bounding limit of 257 MPa .

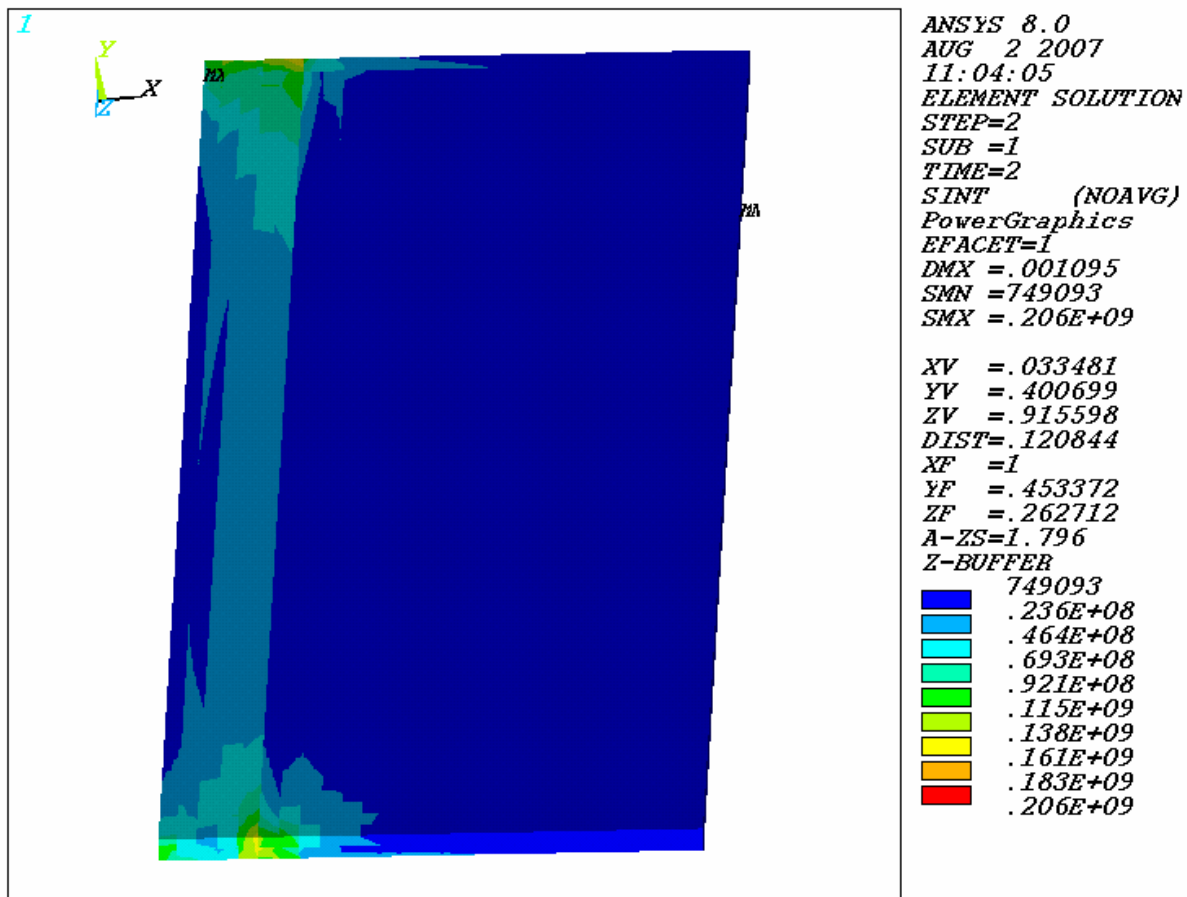


Figure 7-13 Maximum Stress Intensity SI [Pa] of Plate 9 for EP Lift Analysis at 250°C

Figure 7-14 shows the plot of the tensile stress on the surface elements of the WP OCB. The plot result shows that the average maximum tensile stress acting on the surface of WP OCB, 56.8 MPa is less than the bounding limit of 257 MPa.

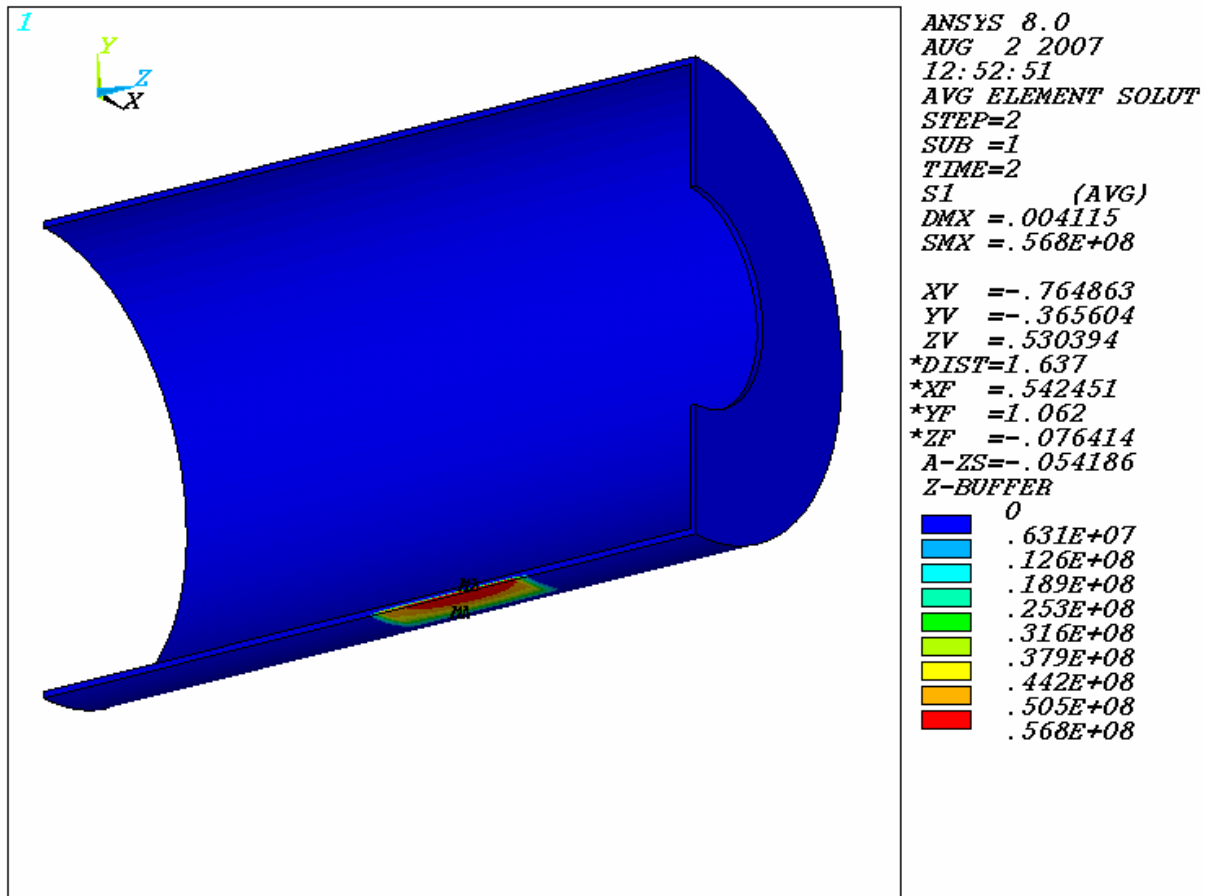


Figure 7-14 Maximum Tensile Stress S1 [Pa] of OCB for EP Lift Analysis at 250 °C

Figure 7-15 shows the average bearing stress of the contact elements of WP OCB. The rows of elements selected across the contact surface of the WP OCB are given in Section 5, Table 5-2, (Attachment I, D:\CD1 of 1\lift250_elist\ocb_250elist.inp). The methodology used to calculate the bearing stress is explained Section 7.1. Magnitude of the average maximum bearing stress (S_b) is 210 MPa, which is less than the allowable design stress intensity limit (S_m), 310 MPa.

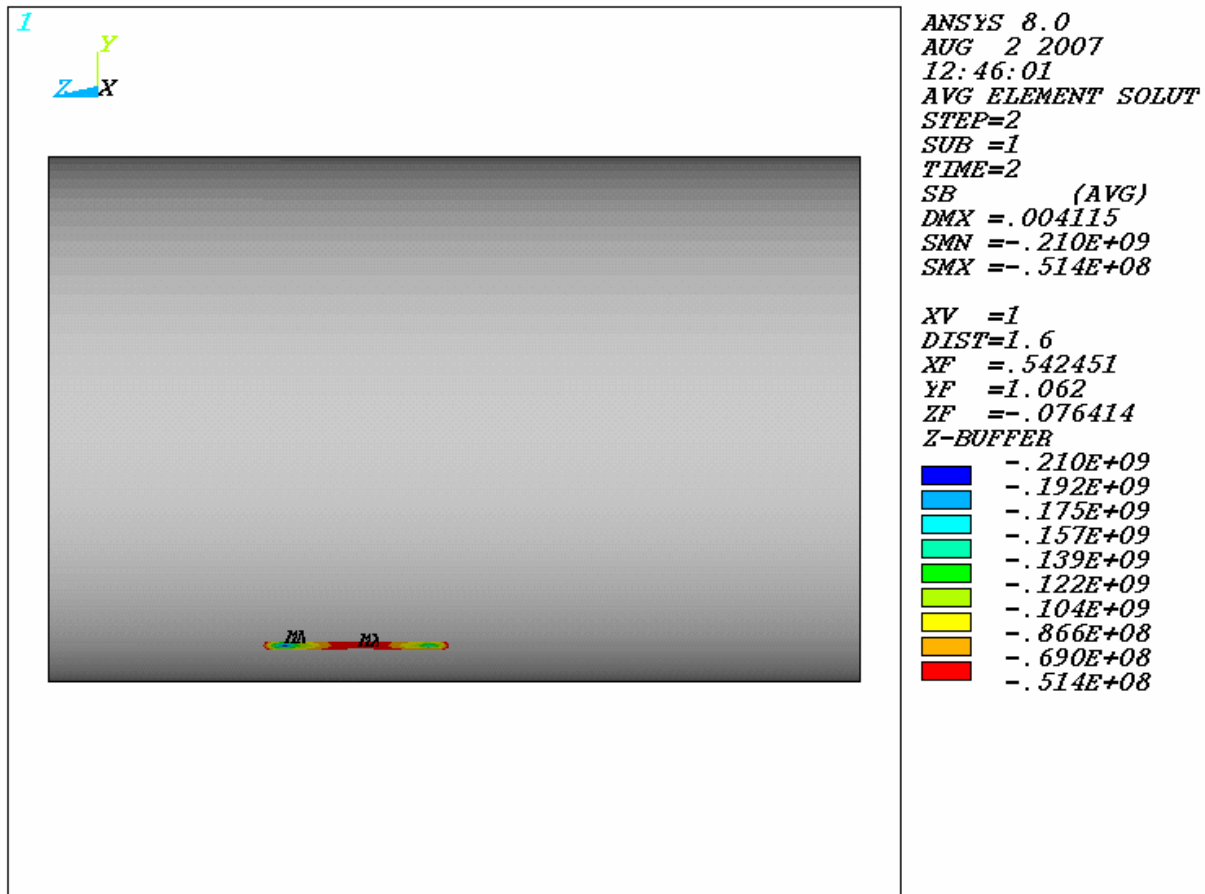


Figure 7-15 Average Bearing Stress S_b [Pa] of OCB for EP Lift Analysis at 250 °C

7.5 DEGRADED EP STATIC ANALYSIS AT RT

Figure 7-16 shows the maximum stress intensity plot of the EP is 204 MPa. This shows that the stress intensity plot of structural components of the EP will be bounded by this value, 204 MPa. Therefore, the maximum stress intensity of the EP is under the allowable design stress intensity limit, 310 MPa.

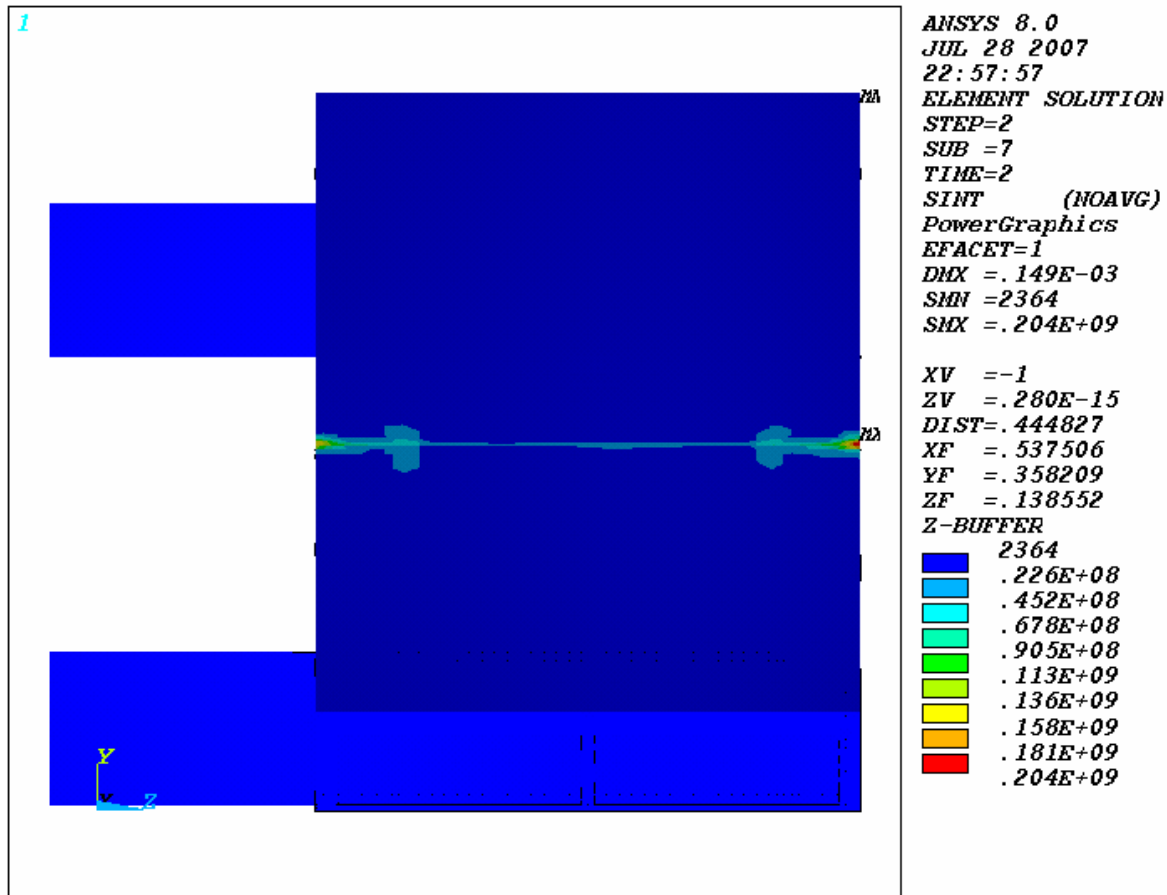
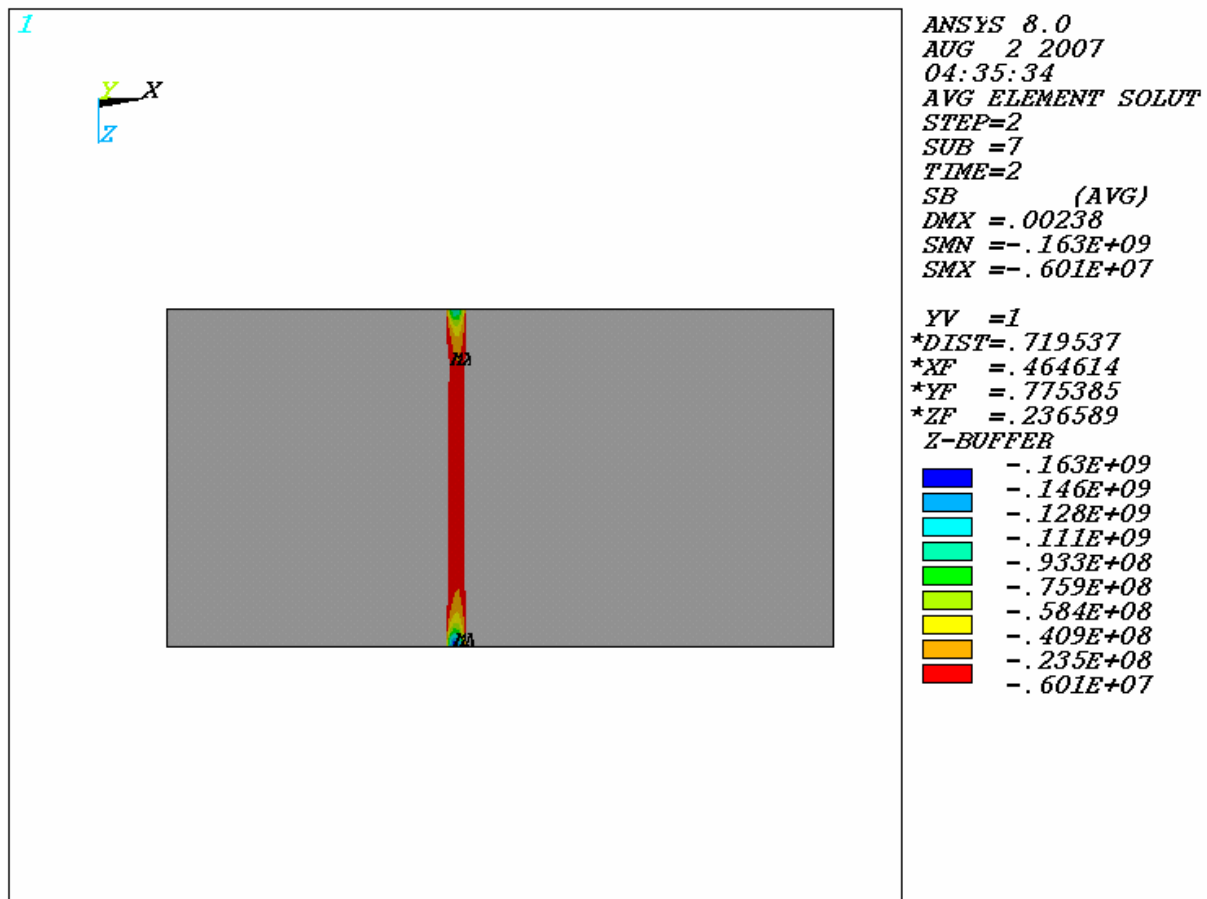
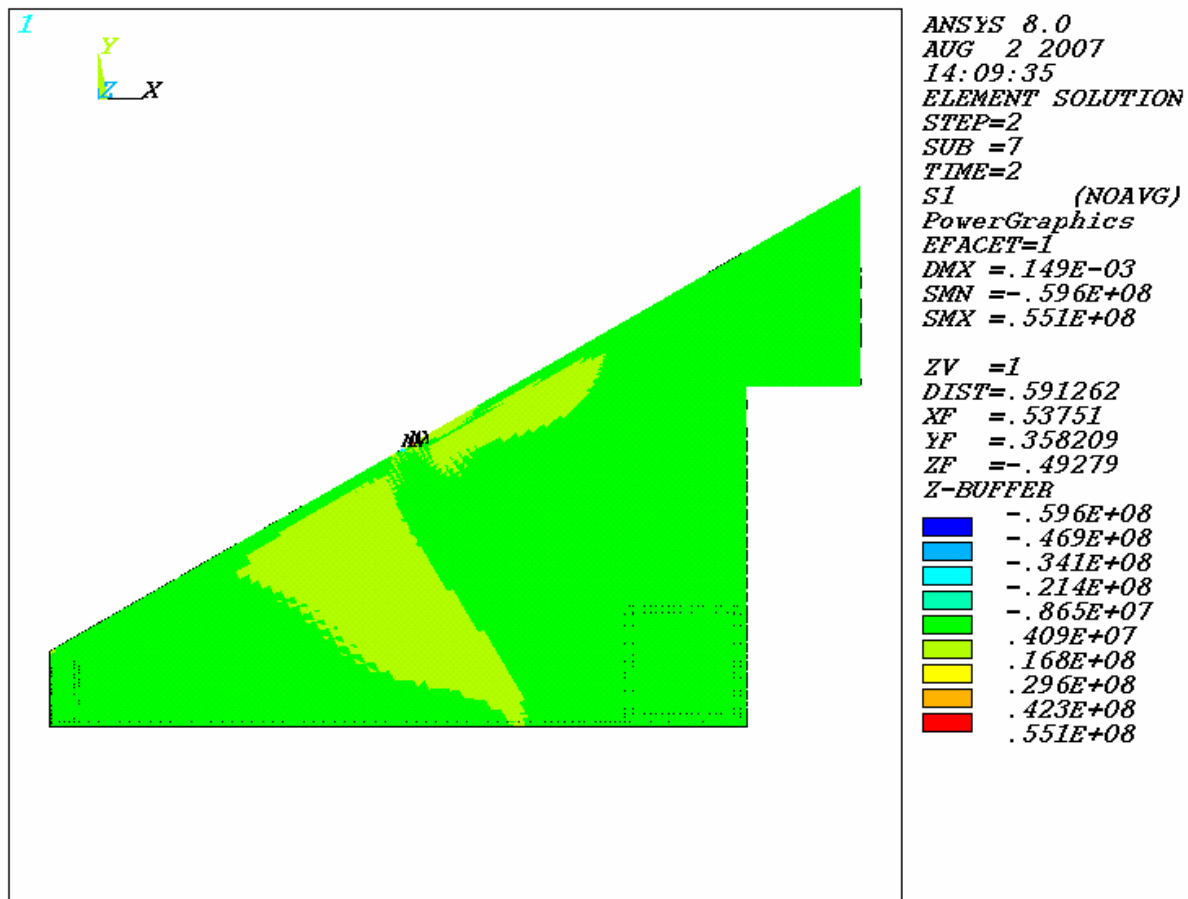
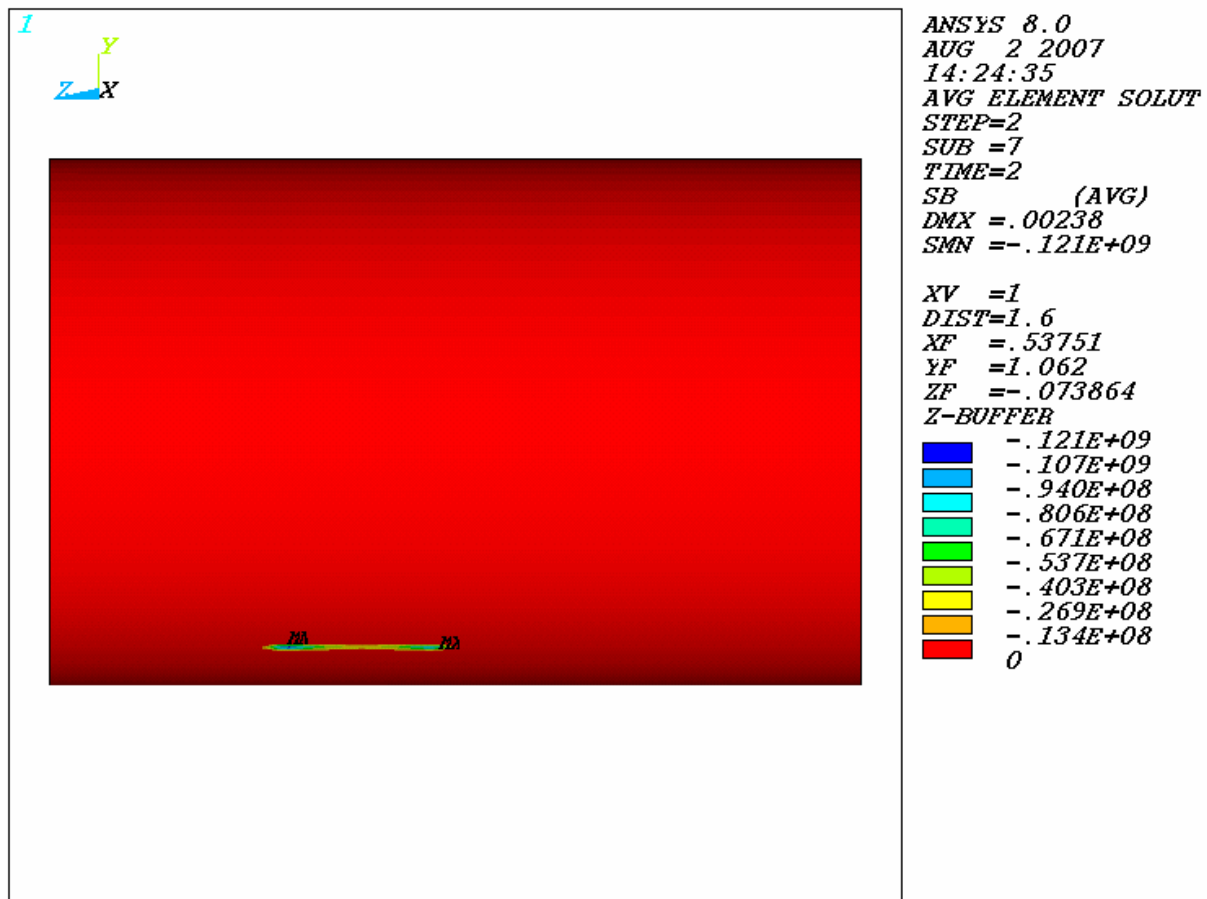


Figure 7-16 Maximum Stress Intensity, S_I [Pa] of the EP for Degraded EP Static Analysis at RT

Figure 7-17 Average Bearing Stress, S_b [Pa] of Plate 6 for Degraded EP Static Analysis at RT

Figure 7-18 Maximum Tensile Stress, $S1$ [Pa] on the EP for the Degraded EP Static Analysis at RT

Figure 7-19 Bearing Stress, S_b [Pa] on the OCB for Degraded EP Static Analysis at RT

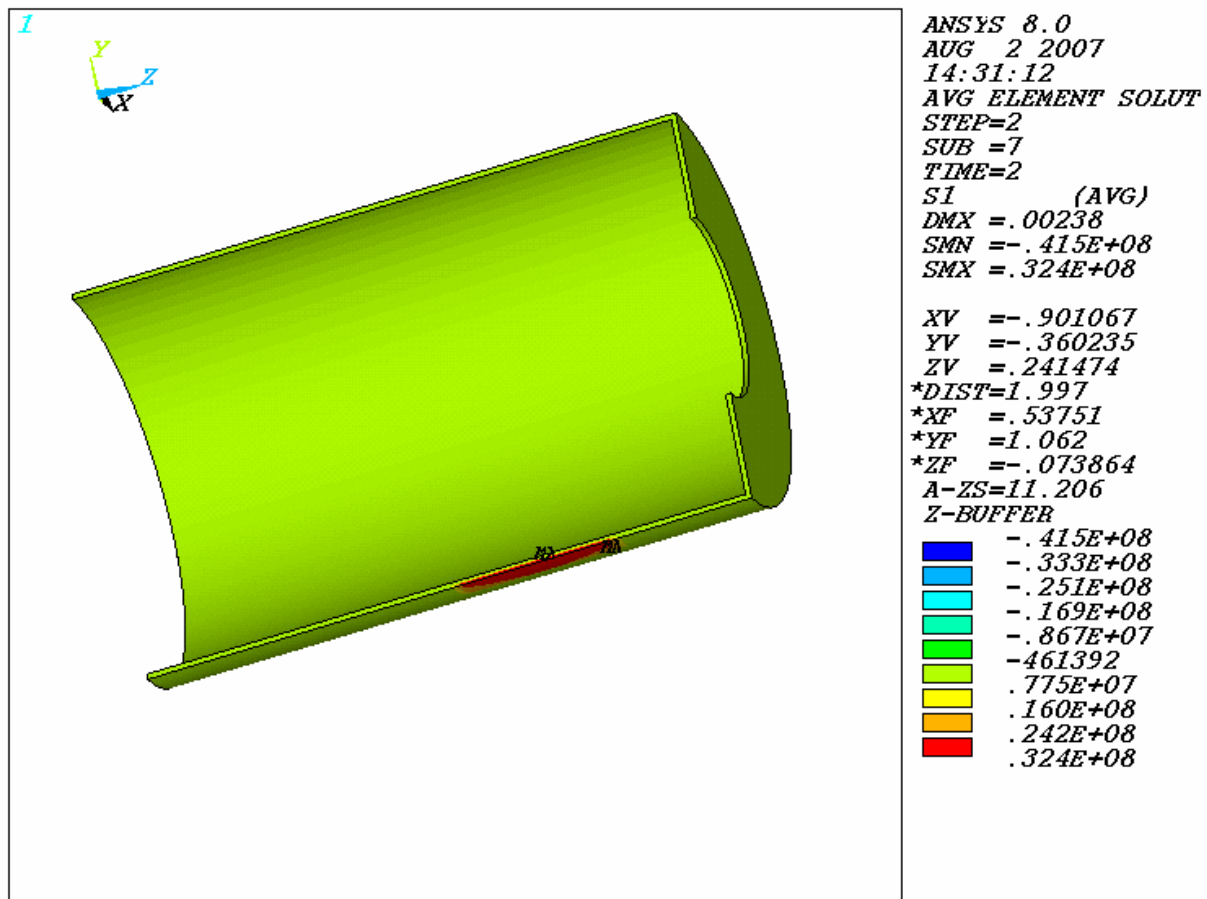


Figure 7-20 Maximum Tensile Stress S1 [Pa] on OCB for Degraded EP Static Analysis at RT

7.6 DEGRADED EP STATIC ANALYSIS AT 150°C

Figure 7-21 shows the maximum stress intensity plot of the EP, which is 201 MPa. This shows that the stress intensity plot of structural components of the EP will be bounded by this value, 201 MPa. Figure 7-21 shows that the maximum stress intensity of the EP is under the allowable design stress intensity limit, 310 MPa.

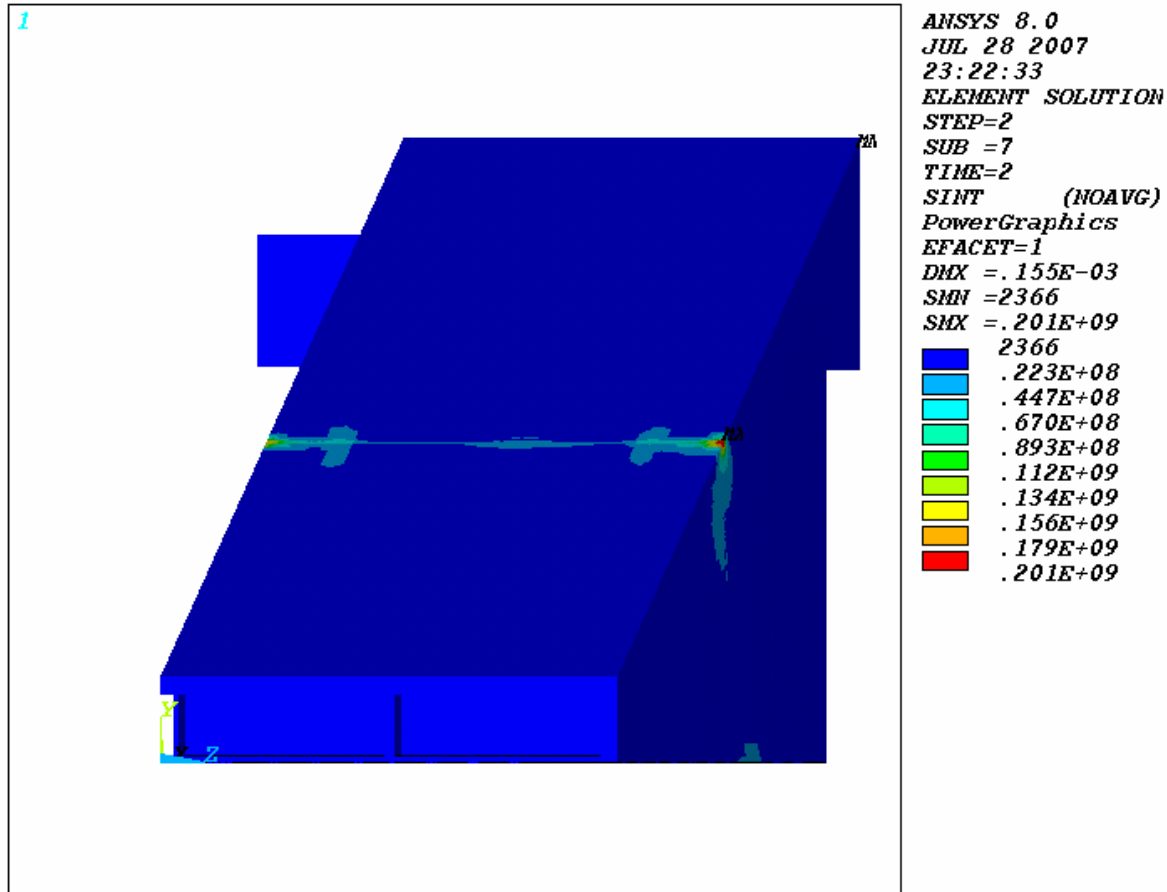
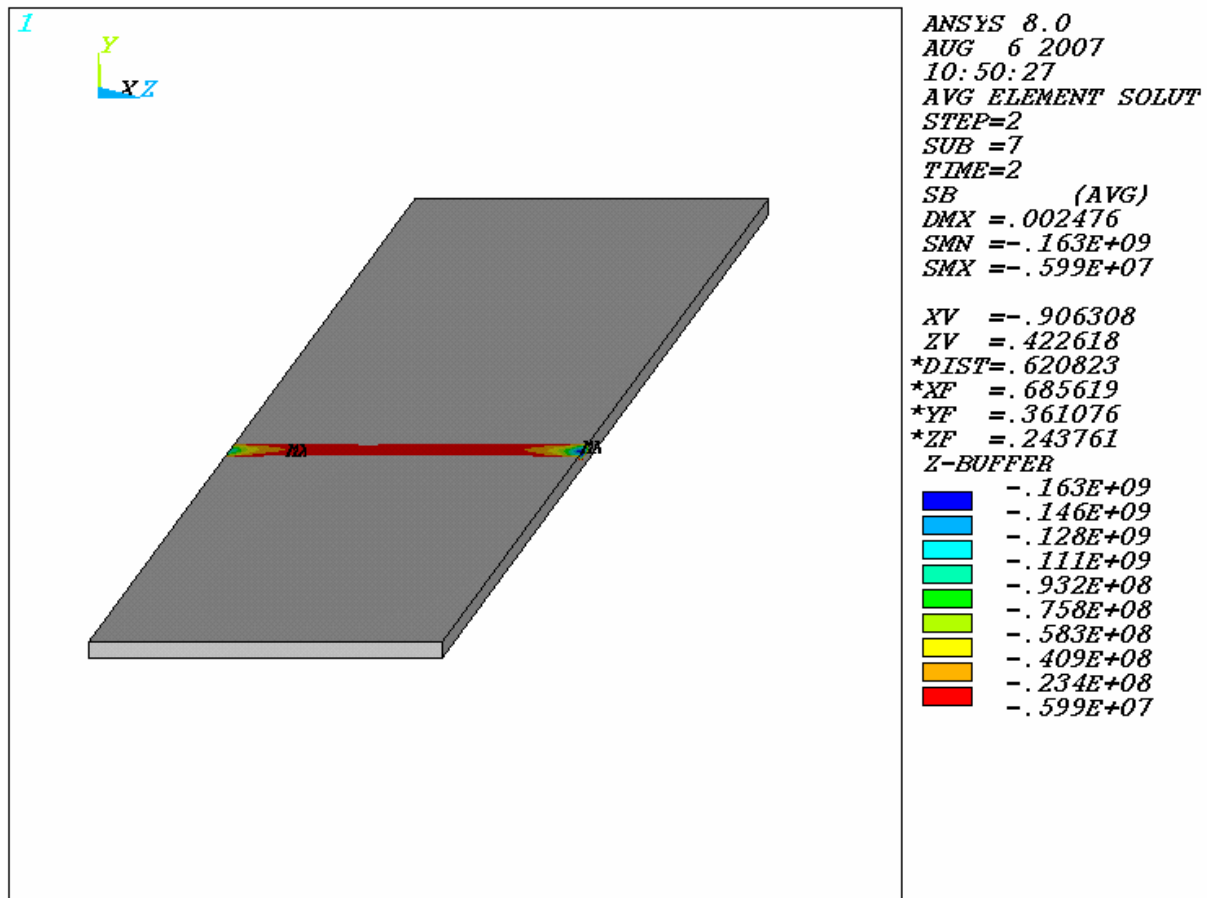


Figure 7-21 Maximum Stress Intensity SI [Pa] of the EP for Degraded EP Static Analysis at 150°C

Figure 7-22 Average Bearing Stress, S_b [Pa] of Plate 6 for Degraded EP Static Analysis at 150°C

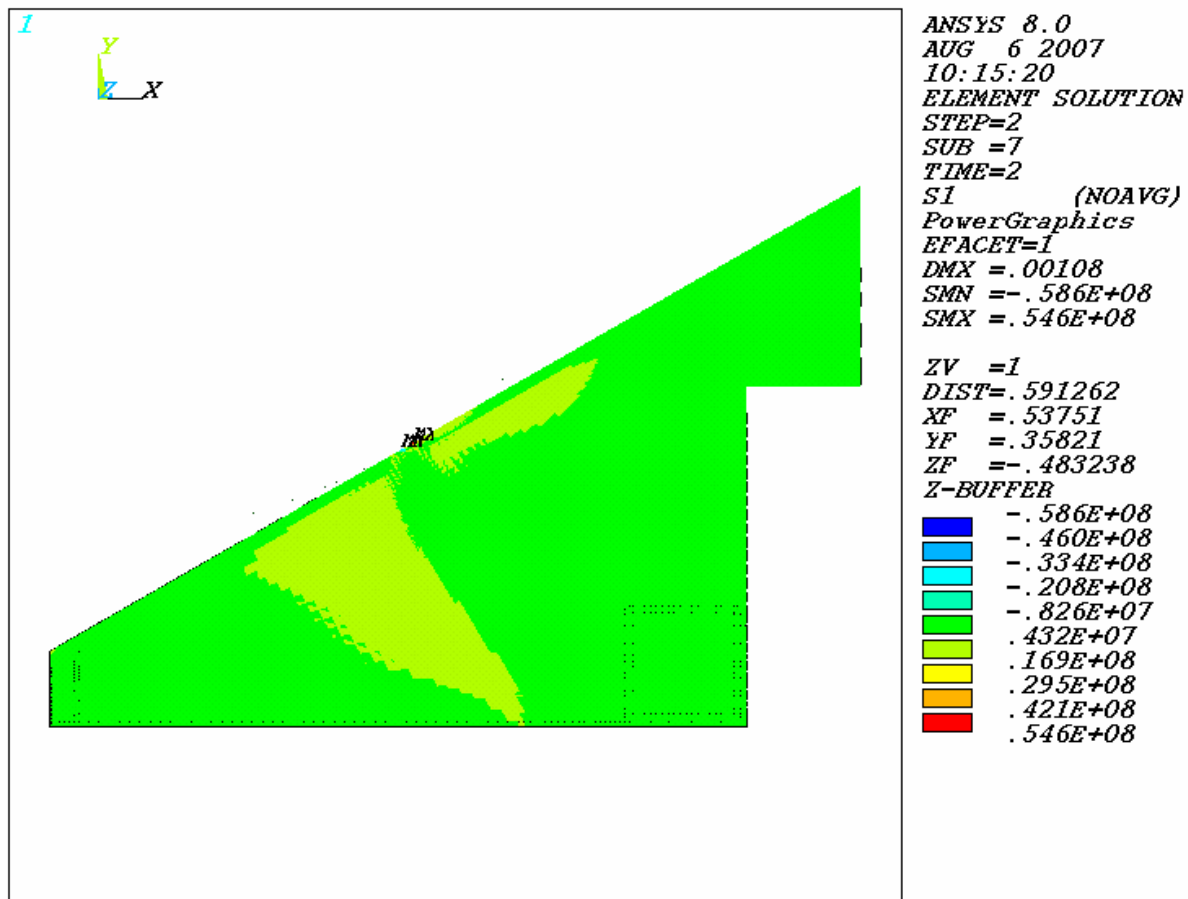


Figure 7-23 Maximum Tensile Stress, $S1$ [Pa] on the EP for the Degraded EP Static Analysis at 150°C

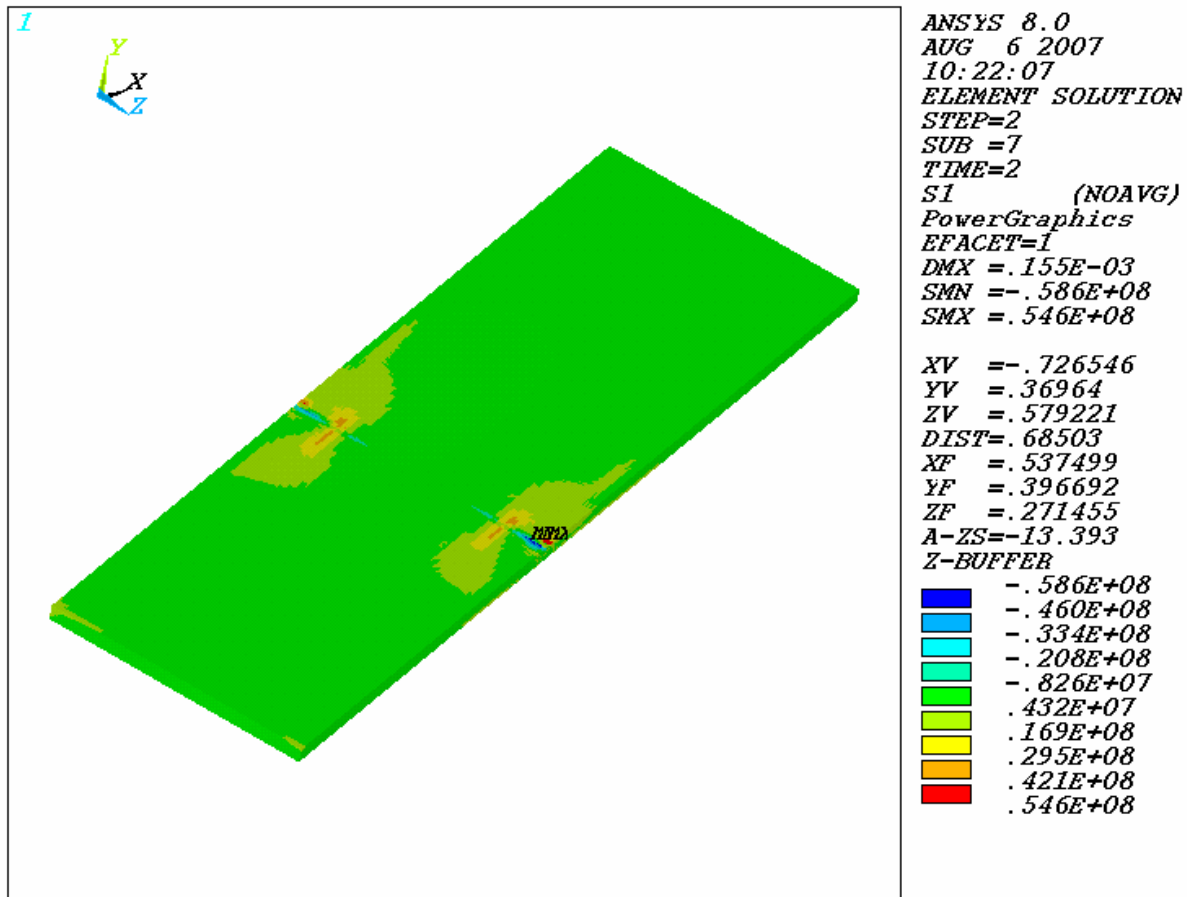


Figure 7-24 Maximum Tensile Stress, S1 [Pa] on Plate 6 for the Degraded EP Static Analysis at 150°C

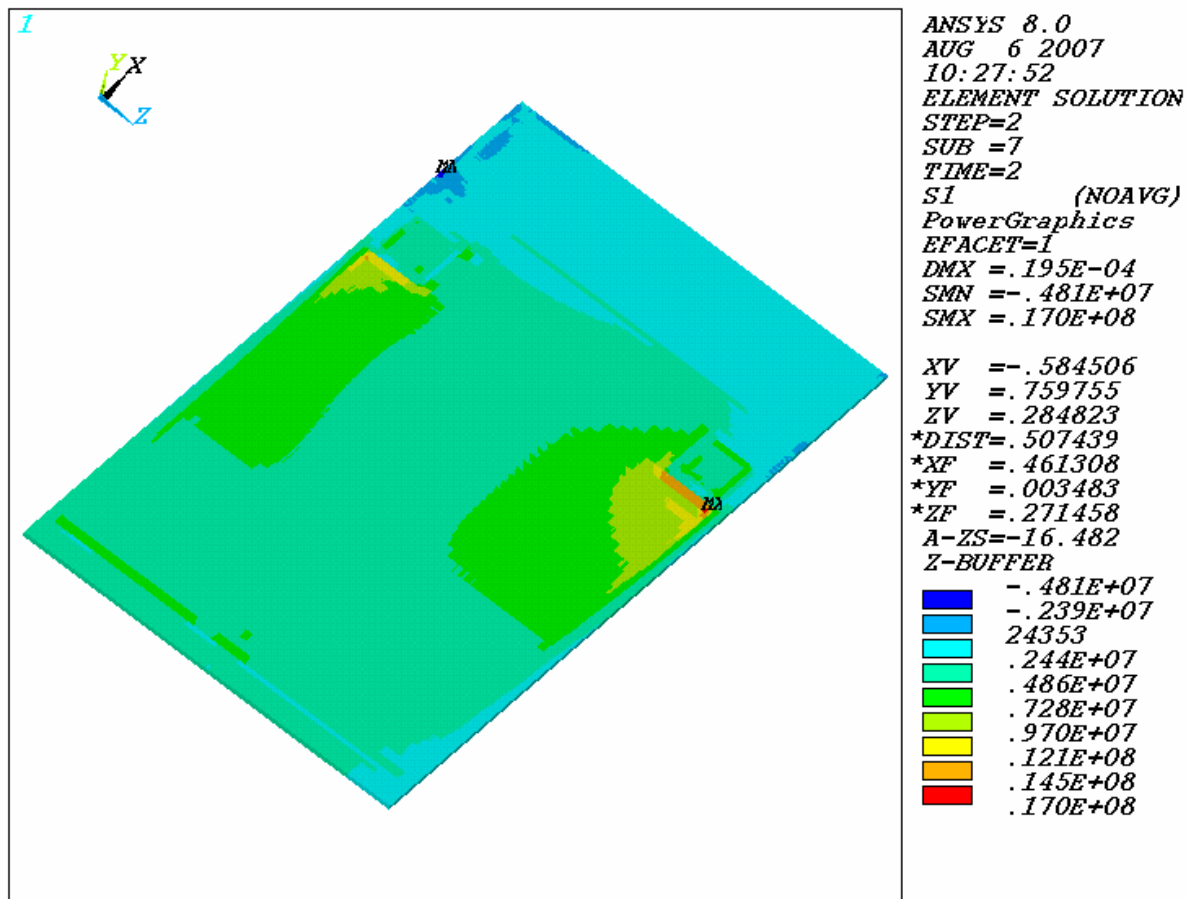
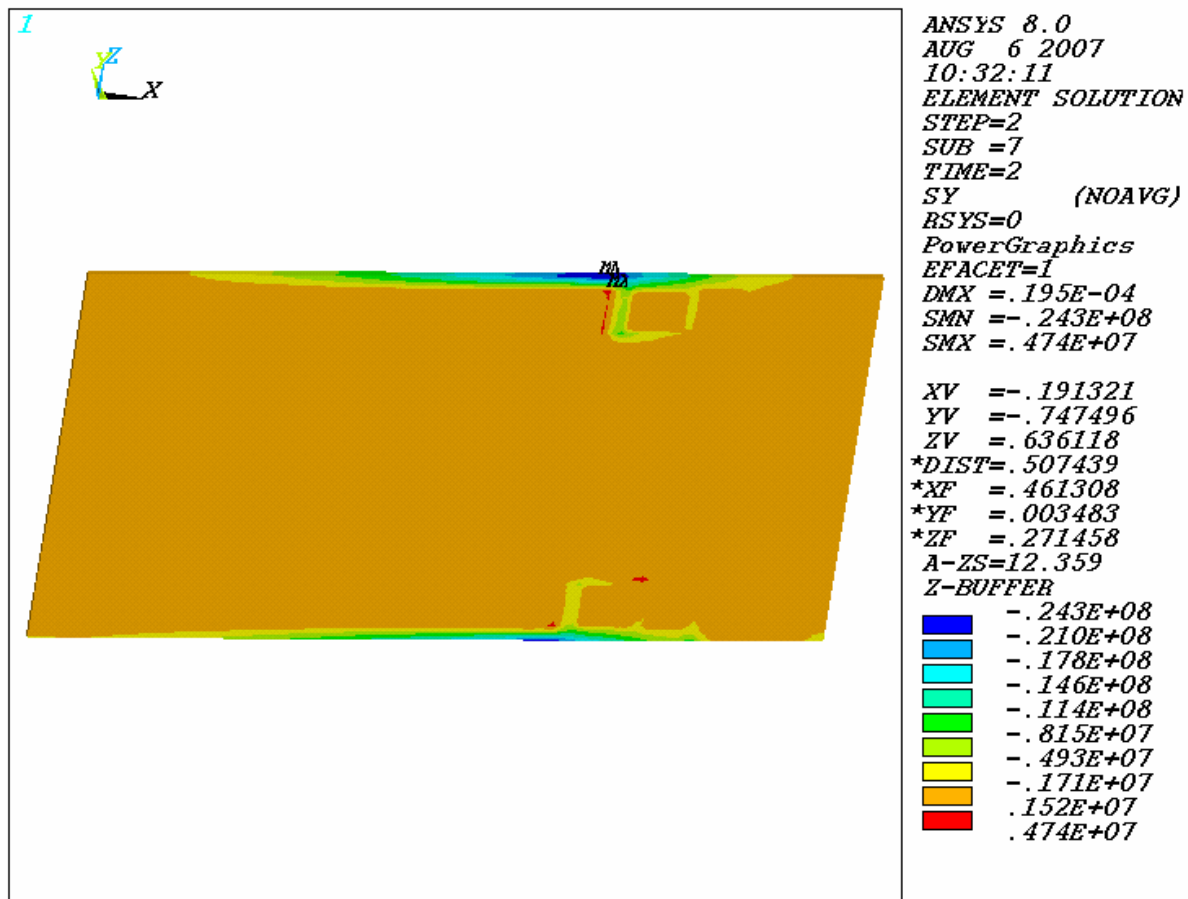


Figure 7-25 Maximum Tensile Stress, $S1$ [Pa] on Plate 1 for the Degraded EP Static Analysis at 150°C

Figure 7-26 Bearing Stress, S_b [Pa] of Plate 1 for Degraded EP Static Analysis at 150°C

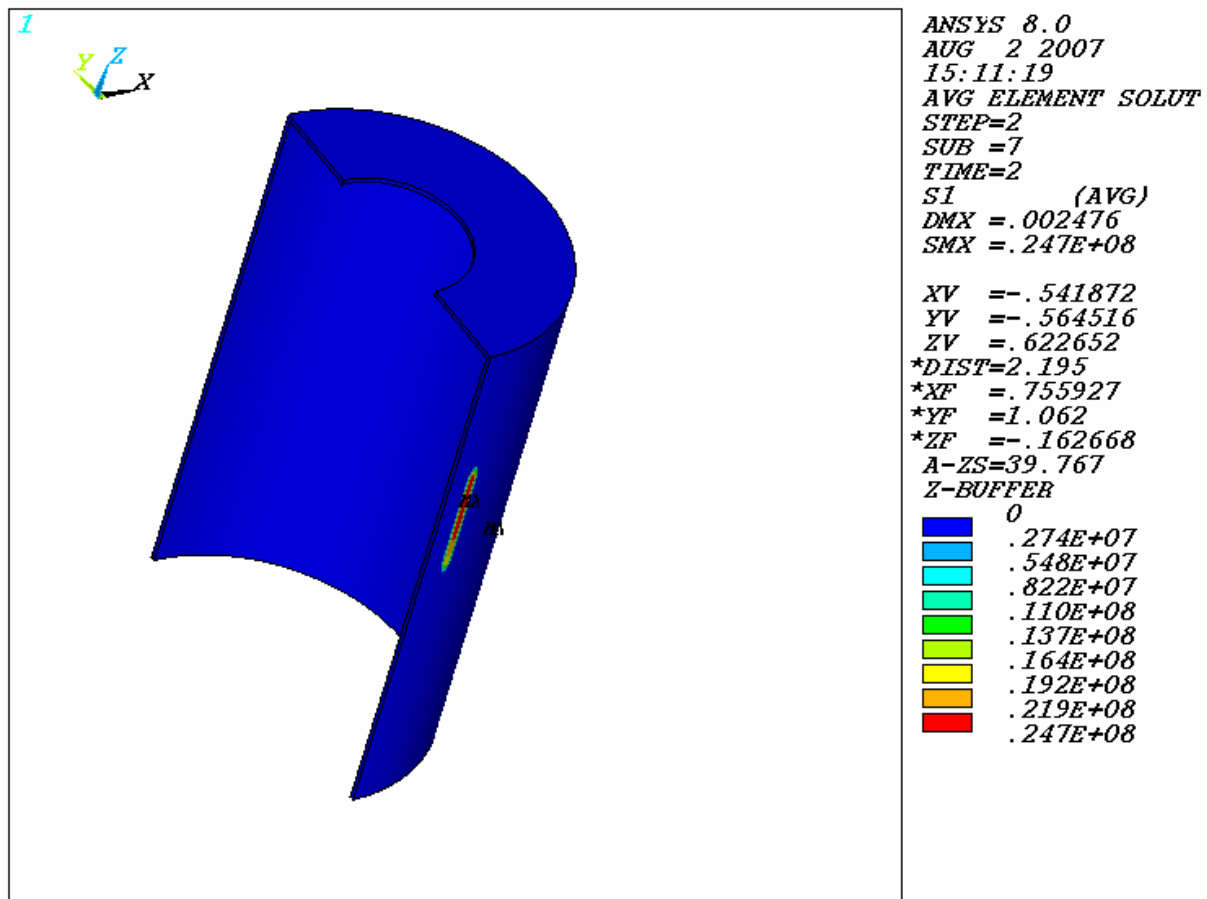


Figure 7-27 Maximum Tensile Stress, S1 [Pa] of OCB for Degraded EP Static Analysis at 150°C

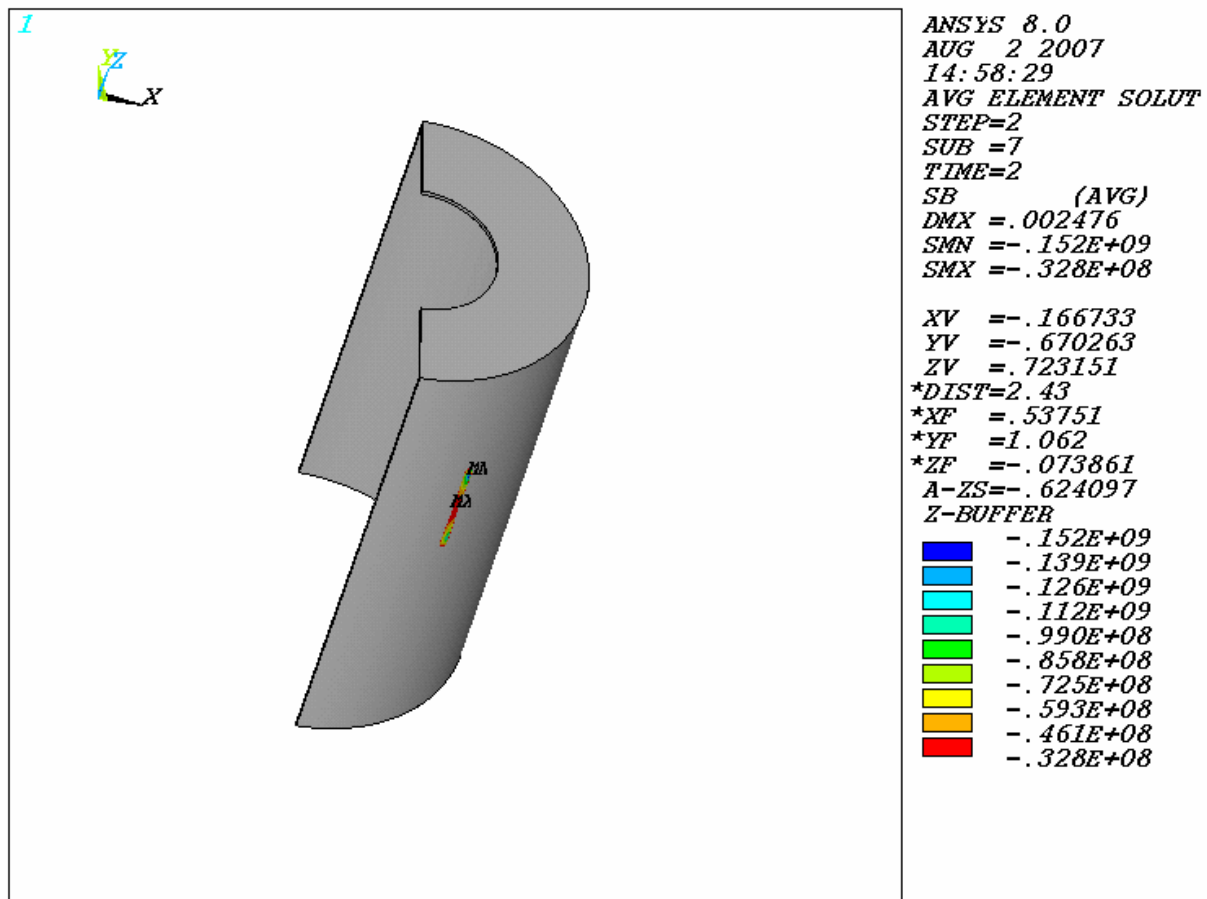


Figure 7-28 Average Bearing Stress, S_b [Pa], of OCB for Degraded EP Static Analysis at 150°C